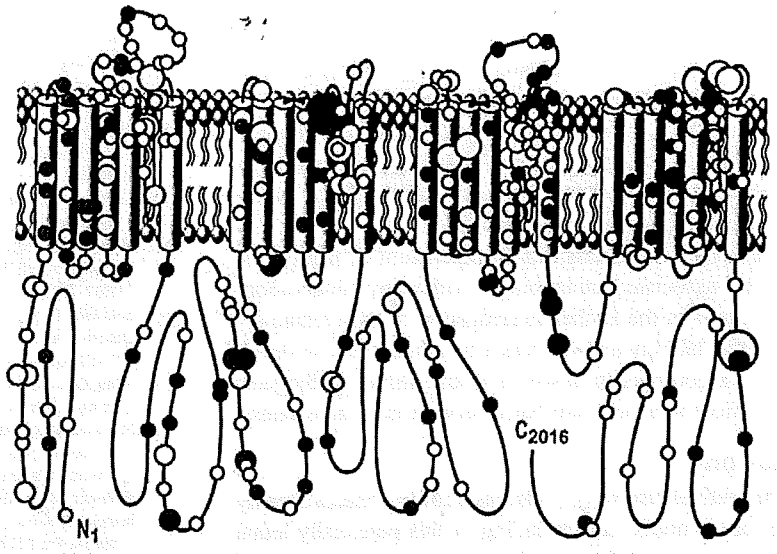

Figure 4 Channel topology of NaV1.5's pore-forming alpha subunit encoded by *SCN5A* and location of putative BrS1-causing mutations. Missense mutations are indicated by white circles, whereas mutations other than missense (i.e., frameshift, deletions, splice-site, etc.) are depicted as gray circles. In addition, 4 different circle sizes are used, with the smallest circle indicating a mutation seen only once; a medium-sized circle for mutations observed in 2, 3, or 4 unrelated patients; a large circle for mutations observed in 5, 6, 7, 8, or 9 patients; and the largest circle indicating those mutations observed in at least 10 unrelated patients.

respectively, were implicated in nearly 11% of BrS cases.[34] Other minor causes of BrS include mutations in the sodium channel beta 1 subunit encoded by *SCN1B* and in a putative beta subunit of the transient outward potassium channel (I_{to}) encoded by *KCNE3*.[35,36] The most recent gene associated with BrS is the *SCN3B*-encoded beta-3 subunit of the cardiac sodium channel.[37]

A number of these minor BrS-susceptibility genes function in part as sodium channel interacting proteins (ChIPs). The cardiac sodium channel is now understood to be a part of a macromolecular complex, with numerous ChIPs regulating its expression, localization, and function. As exemplified by *GPD1L*, *SCN1B*, and *SCN3B*, other genes, which encode other sodium ChIPs whose disruption would portend a loss of function sodium channel phenotype, would warrant examination as candidate BrS disease or disease-modifying genes. These 6 minor BrS-susceptibility genes (*GPD1L*, *CACNA1C*, *CACNB2B*, *SCN1B*, *SCN3B*, and *KCNE3*) have not been examined among the remaining 1,673 *SCN5A*-negative unrelated cases represented in this compendium, but it is predicted that these minor genes will explain <10% of this cohort. Thus, the majority of BrS still remains genetically elusive.

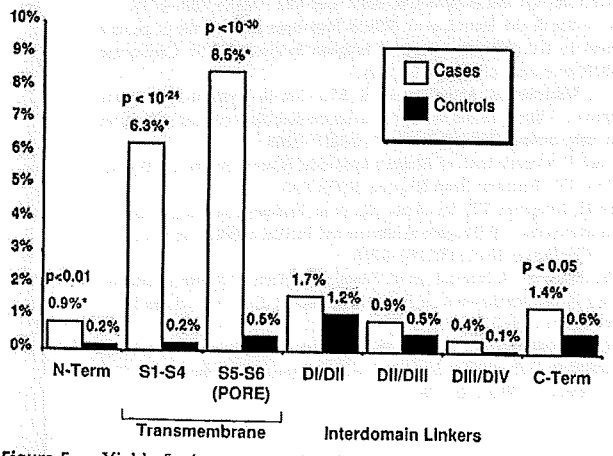

Figure 5 Yield of missense mutations/rare variants in cases and control subjects by location. A comparison of the yield of rare, missense case mutations/control variants in 2,111 cases versus 1,300 control subjects by protein location. * = $p<0.05$.

Study limitations

For the purpose of this compendium of identified mutations, only minimal demographic information from each center's cohort was made available because the focus was on the prevalence, spectrum, and localization of *SCN5A* mutations among suspected cases of BrS rather than an attempt to establish any particular genotype–phenotype correlates. Nevertheless, there is significant clinical value due to the data in aggregate. For example, the rare missense mutations seen numerous times among these cases referred for BrS genetic testing, and still not among the control subjects, indicate high-probability BrS-associated mutations.

Furthermore, despite the lack of clinical information, the physical distribution of mutations/variants among cases and control subjects is very telling, whereby the power in numbers can come from the series of mutations/variants clustering in a region, even if the individual mutations/variants have only been observed rarely. For example, even without cosegregation data or in vitro function analyses, the next rare, nonmissense mutation as well as the next transmembrane-localizing missense mutation represent high-probability pathogenic substrates. Conversely, those rare single amino acid substitutions localizing to the domain I-II and II-III linkers should be buttressed with either clinical cosegregation data or in vitro functional data before being upgraded from this list of possible deleterious mutations to highly probable deleterious mutations.

Additionally, this analysis focused on only identifying coding and splicing region single-nucleotide mutations and small insertion/deletion mutations by molecular techniques that often do not detect larger rearrangements, insertions, and deletions.

SCN5A promoter region mutations, deep intronic mutations, epigenetic methylation mutations, and large genomic rearrangements, all of which could predictably produce a loss-of-function phenotype, would have escaped detection by the mutational analyses performed herein. However, such alterations are quite uncommon when compared with changes in the known coding sequences of the genes.

Despite these limitations, this compendium of nearly 300 distinct BrS-associated mutations provides key observations that may assist in the further interrogation of the cardiac sodium channel biology and serve as a foundation for the development of algorithms to assist in distinguishing pathogenic mutations from similarly rare but otherwise innocuous ones.

Conclusion

Since the sentinel discovery of BrS as a cardiac channelopathy in 1998, our genomic understanding of this potentially lethal disorder has matured from a phase of discovery to one of translational medicine. This international consortium of BrS genetic testing centers has tripled the catalog of possible BrS1-associated mutations with the addition of 200 new mutations to the public domain and has provided a template to draw upon for further genetic testing interpretation and biological inquiry.

References

1. Chen PS, Priori SG. The Brugada syndrome. J Am Coll Cardiol 2008;51:1176–1180.
2. Meregalli PG, Wilde AAM, Tan HL. Pathophysiological mechanisms of Brugada syndrome: depolarization disorder, repolarization disorder, or more? Cardiovasc Res 2005;67:367–378.
3. Antzelevitch C, Brugada P, Borggrefe M, et al. Brugada syndrome: report of the second consensus conference. Heart Rhythm 2005;2:429–440. Erratum: Heart Rhythm 2005;2:905.
4. Tester DJ, Ackerman MJ. Cardiomyopathic and channelopathic causes of sudden unexplained death in infants and children. Annu Rev Med 2009;60:69–84.
5. Brugada P, Brugada J. Right bundle branch block, persistent ST segment elevation and sudden cardiac death: a distinct clinical and electrocardiographic syndrome. A multicenter report. J Am Coll Cardiol 1992;20:1391–1396.
6. Priori SG, Napolitano C, Gasparini M, et al. Clinical and genetic heterogeneity of right bundle branch block and ST-segment elevation syndrome: a prospective evaluation of 52 families. Circulation 2000;102:2509–2515.
7. Priori SG, Napolitano C, Gasparini M, et al. Natural history of Brugada syndrome: insights for risk stratification and management. Circulation 2002;105:1342–1347.
8. Schulze-Bahr E, Eckardt L, Breithardt G, et al. Sodium channel gene (SCN5A) mutations in 44 index patients with Brugada syndrome: different incidences in familial and sporadic disease. Hum Mutat 2003;21:651–652. Erratum: Hum Mutat 2005;26:61.
9. Remme CA, Wilde AAM. SCN5A overlap syndromes: no end to disease complexity? [Comment.] Europace 2008;10:1253–255.
10. Zimmer T, Surber R. SCN5A channelopathies—an update on mutations and mechanisms. Prog Biophys Mol Biol 2008;98(2–3):120–136.
11. Ackerman MJ, Splawski I, Makielski JC, et al. Spectrum and prevalence of cardiac sodium channel variants among black, white, Asian, and Hispanic individuals: implications for arrhythmogenic susceptibility and Brugada/long QT syndrome genetic testing (see Comment). Heart Rhythm 2004;1:600–607.
12. Spiegelman JI, Mindrinos MN, Oefner PJ. High-accuracy DNA sequence variation screening by DHPLC. BioTechniques 2000;29:1084–1092.
13. Kapa S, Tester DJ, Salisbury BA, et al. Genetic testing for long QT syndrome—distinguishing pathogenic mutations from benign variants. Circulation 2009;120(18):1752–1760.
14. den Dunnen JT, Antonarakis SE. Nomenclature for the description of human sequence variations. Hum Genet 2001;109:121–124.
15. Murray A, Donger C, Fenske C, et al. Splicing mutations in KCNQ1: a mutation hot spot at codon 344 that produces in frame transcripts. Circulation 1999;100:1077–1084.
16. Zhuang Y, Weiner AM. A compensatory base change in U1 snRNA suppresses a 5′ splice site mutation. Cell 1986;46:827–835.
17. Rogan PK, Svojanovsky S, Leeder JS. Information theory-based analysis of CYP2C19, CYP2D6 and CYP3A5 splicing mutations. Pharmacogenetics 2003;13:207–218.
18. Splawski I, Shen J, Timothy K, Vincent GM, Lehmann MH, Keating MT. Genomic structure of three long QT syndrome genes: KVLQT1, HERG, and KCNE1. Genomics 1998;51:86–97.
19. Wang Q, Li Z, Shen J, Keating MT. Genomic organization of the human SCN5A gene encoding the cardiac sodium channel. Genomics 1996;34:9–16.
20. Neyroud N, Richard P, Vignier N, et al. Genomic organization of the KCNQ1 K+ channel gene and identification of C-terminal mutations in the long-QT syndrome. Circ Res 1999;84:290–297.
21. Wehrens XHT, Rossenbacker T, Jongbloed RJ, et al. A novel mutation L619F in the cardiac Na+ channel SCN5A associated with long-QT syndrome (LQT3): a role for the I-II linker in inactivation gating. Hum Mutat 2003;21:552.
22. Ruan Y, Liu N, Bloise R, Napolitano C, Priori SG. Gating properties of SCN5A mutations and the response to mexiletine in long-QT syndrome type 3 patients. Circulation 2007;116:1137–1144.
23. Kambouris NG, Nuss HB, Johns DC, Tomaselli GF, Marban E, Balser JR. Phenotypic characterization of a novel long-QT syndrome mutation (R1623Q) in the cardiac sodium channel. Circulation 1998;97:640–644.
24. Wei J, Wang DW, Alings M, et al. Congenital long-QT syndrome caused by a novel mutation in a conserved acidic domain of the cardiac Na+ channel. Circulation 1999;99:3165–3171.
25. Yang P, Kanki H, Drolet B, et al. Allelic variants in long-QT disease genes in patients with drug-associated torsades de pointes. Circulation 2002;105:1943–1948.
26. Chen Q, Kirsch GE, Zhang D, et al. Genetic basis and molecular mechanism for idiopathic ventricular fibrillation. Nature 1998;392:293–296.
27. Kapplinger JD, Tester DJ, Salisbury BA, et al. Spectrum and prevalence of mutations from the first 2500 consecutive unrelated patients referred for the *FAMILION*® long QT syndrome genetic test. Heart Rhythm 2009;6:1297–1303.
28. Tester DJ, Will ML, Haglund CM, Ackerman MJ. Compendium of cardiac channel mutations in 541 consecutive unrelated patients referred for long QT syndrome genetic testing. Heart Rhythm 2005;2:507–517.
29. Meregalli PG, Tan HL, Probst V, et al. Type of SCN5A mutation determines clinical severity and degree of conduction slowing in loss-of-function sodium channelopathies. Heart Rhythm 2009;6:341–348.
30. Makita N, Behr E, Shimizu W, et al. The E1784K mutation in SCN5A is associated with mixed clinical phenotype of type 3 long QT syndrome. J Clin Invest 2008;118:2219–2229.
31. Bezzina C, Veldkamp MW, van den Berg MP, et al. A single Na^+ channel mutation causing both long-QT and brugada syndromes. Circ Res 1999;85:1206–1213.
32. Probst V, Wilde AAM, Barc J, et al. *SCN5A* Mutations and the role of genetic background in the pathophysiology of brugada syndrome. Circ Cardiovasc Genet 2009; accepted manuscript, in press.
33. London B, Michalec M, Mehdi H, et al. Mutation in glycerol-3-phosphate dehydrogenase 1 like gene (GPD1-L) decreases cardiac Na+ current and causes inherited arrhythmias. Circulation 2007;116:2260–2268.
34. Antzelevitch C. Genetic basis of Brugada syndrome [Comment]. Heart Rhythm 2007;4:756–757. Erratum: Heart Rhythm 2007;4:990.
35. Watanabe H, Koopman TT, Scouarnec SL, et al. Sodium channel β1 subunit mutations associated with Brugada syndrome and cardiac conduction disease in humans. J Clin Invest 2008;118:2260–2268.
36. Delpon E, Cordeiro JM, Nunez L, et al. Functional effects of KCNE3 mutation and its role in the development of Brugada syndrome. Circ Arrhythmia Electrophysiol 2008;1:209–218.
37. Hu S, Barajas-Martinez H, Burashnikove E, et al. A mutation in the β3 subunit of the cardiac sodium channel associated with Brugada ECG phenotype. Circ Cardiovasc Genet 2009;2:270–278.

KCNE2 modulation of Kv4.3 current and its potential role in fatal rhythm disorders

Jie Wu, PhD,* Wataru Shimizu, MD, PhD,† Wei-Guang Ding, MD, PhD,‡ Seiko Ohno, MD, PhD,§ Futoshi Toyoda, PhD,‡ Hideki Itoh, MD, PhD,¶ Wei-Jin Zang, MD, PhD,* Yoshihiro Miyamoto, MD, PhD,‖ Shiro Kamakura, MD, PhD,† Hiroshi Matsuura, MD, PhD,‡ Koonlawee Nademanee, MD, FACC,# Josep Brugada, MD,** Pedro Brugada, MD,†† Ramon Brugada, MD, PhD, FACC,‡‡ Matteo Vatta, PhD,§§¶¶ Jeffrey A. Towbin, MD, FAAP, FACC,§§ Charles Antzelevitch, PhD, FACC, FAHA, FHRS,‖‖ Minoru Horie, MD, PhD¶

*From the *Pharmacology Department, Medical School of Xi'an Jiaotong University. Xi'an, Shaanxi, China, †Division of Cardiology, Department of Internal Medicine, National Cardiovascular Center, Suita, Japan, ‡Department of Physiology, Shiga University of Medical Science, Ohtsu, Japan, §Department of Cardiovascular Medicine, Kyoto University of Graduate School of Medicine, Kyoto, Japan, ¶Department of Cardiovascular Medicine, Shiga University of Medical Science, Shiga, Japan, ‖Laboratory of Molecular Genetics, National Cardiovascular Center, Suita, Japan, #Department of Medicine (Cardiology), University of Southern California, Los Angeles, California, **Cardiovascular Institute, Hospital Clinic, University of Barcelona, Barcelona, Spain, ††Heart Rhythm Management Centre, Free University of Brussels (UZ Brussel) VUB, Brussels, Belgium, ‡‡School of Medicine, Cardiovascular Genetics Center, University of Girona, Girona, Spain, §§Departments of Pediatrics, Baylor College of Medicine, Houston, Texas, ¶¶Department of Molecular Physiology and Biophysics, Baylor College of Medicine, Houston, Texas, and ‖‖Masonic Medical Research Laboratory, Utica, New York.*

BACKGROUND The transient outward current I_{to} is of critical importance in regulating myocardial electrical properties during the very early phase of the action potential. The auxiliary β subunit *KCNE2* recently was shown to modulate I_{to}.

OBJECTIVE The purpose of this study was to examine the contributions of *KCNE2* and its two published variants (M54T, I57T) to I_{to}.

METHODS The functional interaction between Kv4.3 (α subunit of human I_{to}) and wild-type (WT), M54T, and I57T *KCNE2*, expressed in a heterologous cell line, was studied using patch-clamp techniques.

RESULTS Compared to expression of Kv4.3 alone, co-expression of WT *KCNE2* significantly reduced peak current density, slowed the rate of inactivation, and caused a positive shift of voltage dependence of steady-state inactivation curve. These modifications rendered Kv4.3 channels more similar to native cardiac I_{to}. Both M54T and I57T variants significantly increased I_{to} current density and slowed the inactivation rate compared with WT *KCNE2*. Moreover, both variants accelerated the recovery from inactivation.

CONCLUSION The study results suggest that *KCNE2* plays a critical role in the normal function of the native I_{to} channel complex in human heart and that M54T and I57T variants lead to a gain of function of I_{to}, which may contribute to generating potential arrhythmogeneity and pathogenesis for inherited fatal rhythm disorders.

KEYWORDS Cardiac arrhythmia; M54T variation; I57T variation; *KCNE2*; Kv4.3; Sudden cardiac death

ABBREVIATIONS CHO = Chinese hamster ovary; **HERG** = human ether-a-go-go related gene; **WT** = wild type

(Heart Rhythm 2010;7:199–205)

Introduction

Classic voltage-gated K^+ channels consist of four pore-forming (α) subunits that contain the voltage sensor and ion selectivity filter[1,2] and accessory regulating (β) subunits.[3] *KCNE* family genes encode several kinds of β subunits consisting of single transmembrane-domain peptides that co-assemble with α subunits to modulate ion selectivity, gating kinetics, second messenger regulation, and the pharmacology of K^+ channels. Association of the *KCNE1* product minK with the α subunit Kv7.1 encoding *KCNQ1* forms the slowly activating delayed rectifier K^+ current I_{Ks} in the heart.[4,5] In contrast, association of the *KCNE2* product MiRP1 with the human ether-a-go-go related gene (HERG) forms the cardiac rapid delayed rectifier K^+ current I_{Kr}.[6]

The first two authors contributed equally to the original concept and the authorship of this study. This study was supported by grants from the Ministry of Education, Culture, Sports, Science, Technology Leading Project for Biosimulation to Dr. Horie; Health Sciences Research grants (H18-Research on Human Genome-002) from the Ministry of Health, Labour and Welfare, Japan to Drs. Shimizu and Horie; the National Natural Science Foundation of China (Key Program, No.30930105; General Program, No. 30873058, 30770785) and the National Basic Research Program of China (973 Program, No. 2007CB512005) and CMB Distinguished Professorships Award (No. F510000/G16916404) to Dr. Zang; and National Institutes of Health Grant HL47678 and Free and Accepted Masons of New York State and Florida to Dr. Antzelevitch. **Address reprint requests and correspondence:** Dr. Minoru Horie, Department of Cardiovascular and Respiratory Medicine, Shiga University of Medical Science, Otsu, Shiga 520-2192, Japan. E-mail address: horie@belle.shiga-med.ac.jp. (Received August 20, 2009; accepted October 7, 2009.)

1547-5271/$ -see front matter doi:10.1016/j.hrthm.2009.10.012

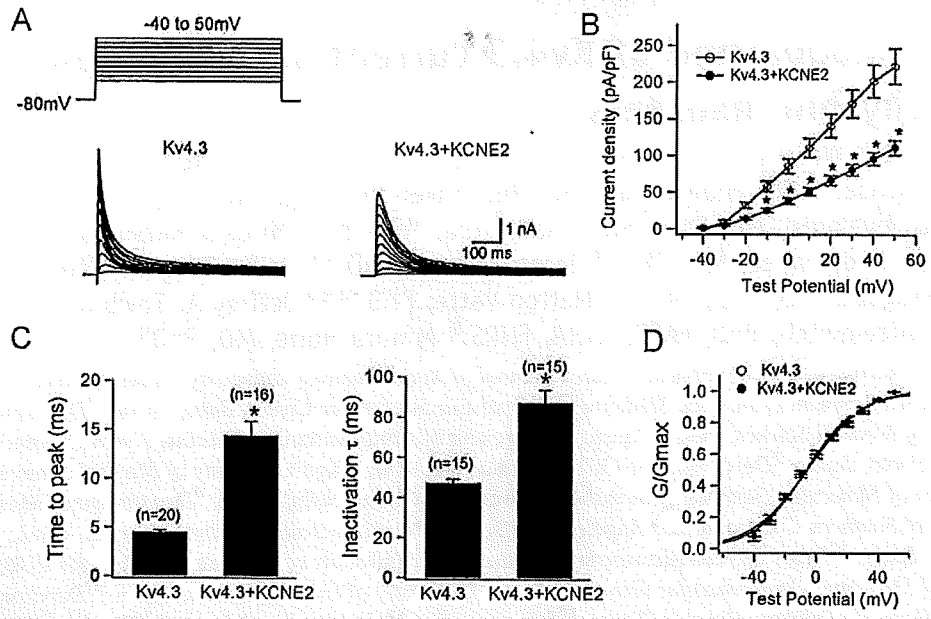

Figure 1 *KCNE2* co-expression with Kv4.3 produces smaller I_{to}-like currents with slower activation/inactivation kinetics. **A:** Representative current traces recorded from Chinese hamster ovary (CHO) cells expressing Kv4.3 (**left**) and Kv4.3 + *KCNE2* (**right**). As shown in the inset in panel A, depolarizing step pulses of 1-second duration were introduced from a holding potential of −80 mV to potentials ranging from −40 to +50 mV in 10-mV increments. **B:** Current–voltage relationship curve showing peak current densities in the absence and presence of co-transfected *KCNE2* (*P <.05 vs Kv4.3). **C:** Bar graphs showing the kinetic properties of reconstituted channel currents: time to peak of activation course (**left**) and inactivation time constants (**right**) measured using test potential to +20 mV (*P <.05 vs Kv4.3). Numbers in parentheses indicate numbers of experiments. **D:** Normalized conductance–voltage relationship for peak outward current of Kv4.3 and Kv4.3 + *KCNE2* channels.

Abbott et al reported that three *KCNE2* variants (Q9E, M54T, I57T) caused a loss of function in I_{Kr} and thereby were associated with the congenital or drug-induced long QT syndrome.[6,7] However, the reported QTc values in two index patients with M54T and I57T variants, both located in the transmembrane segment of MiRP1, were only mildly prolonged (390–500 ms and 470 ms).[6] We recently identified the same missense *KCNE2* variant, I57T, in which isoleucine was replaced by threonine at codon 57, in three unrelated probands showing a Brugada type 1 ECG. These findings are difficult to explain on the basis of a loss of function in I_{Kr}, thus leading us to explore other mechanisms.

Recent studies have demonstrated that interaction between α and β subunits (*KCNE*s) of voltage-gated K^+ channel is more promiscuous; for example, MiRP1 has been shown to interact with Kv7.1,[8–10] HCN1,[11] Kv2.1,[12] and Kv4.2.[13] These studies suggest that MiRP1 may also co-associate with Kv4.3 and contribute to the function of transient outward current (I_{to}) channels.[14] Indeed, a recent study reported that I_{to} is diminished in *kcne2* (–/–) mice.[15]

In the human heart, I_{to} currents are of critical importance in regulating myocardial electrical properties during the very early phase of the action potential and are thought to be central to the pathogenesis of Brugada-type ECG manifestations.[16] Antzelevitch et al demonstrated that a gain of function in I_{to} secondary to a mutation in *KCNE3* contributes to a Brugada phenotype by interacting with Kv4.3 and thereby promoting arrhythmogenicity.[14]

We hypothesized that mutations in *KCNE2* may have similar actions and characterize the functional consequences of interaction of wild-type (WT) and two mutant (I57T, M54T) MiRP1 with Kv4.3[17,18] using heterologous co-expression of these α and β subunits in Chinese hamster ovary (CHO) cells.

Methods

Heterologous expression of hKv4.3 and β subunits in CHO cells

Full-length cDNA fragment of *KCNE2* in pCR3.1 vector[10] was subcloned into pIRES-CD8 vector. This expression vector is useful in cell selection for later electrophysiologic study (see below). Two *KCNE2* mutants (M54T, I57T) were constructed using a Quick Change II XL site-directed mutagenesis kit according to the manufacturer's instructions (Stratagene, La Jolla, CA, USA) and subcloned to the same vector. Two *KCNE2* mutants were fully sequenced (ABI3100x, Applied Biosystems, Foster City, CA, USA) to ensure fidelity. Full-length cDNA encoding the short isoform of human Kv4.3 subcloned into the pIRES-GFP (Clontech, Palo Alto, CA, USA) expression vector was kindly provided by Dr. G.F. Tomaselli (Johns Hopkins University). Full-length cDNA encoding Kv channel-interacting protein (*KCNIP2*) subcloned into the PCMV-IRS expression vector was a kind gift from Dr. G.-N. Tseng (Virginia Commonwealth University). *KCND3* was transiently transfected into CHO cells together with *KCNE2* (or M54T or I57T) cDNA at equimolar ratio (*KCND3* 1.5 μg,

Table 1 Effects of *KCNE2* on Kv4.3 and Kv4.3 + KChIP2b

Parameter	Kv4.3	Kv4.3 *KCNE2*	Kv4.3 KChIP2b	Kv4.3 KChIP2b *KCNE2*
Current density at +20 mV (pA/pF)	142.0 ± 16.0 (n = 12)	66.0 ± 6.6* (n = 12)	191.5 ± 33.8 (n = 15)	77.8 ± 5.9† (n = 20)
Steady-state activation ($V_{0.5}$ in mV)	−6.5 ± 2.1 (n = 9)	−5.5 ± 1.7 (n = 11)	−7.5 ± 1.7 (n = 8)	−7.4 ± 1.4 (n = 8)
Steady-state inactivation ($V_{0.5}$ in mV)	−46.0 ± 1.3 (n = 10)	−40.8 ± 1.7* (n = 8)	−49.8 ± 1.4 (n = 7)	−44.5 ± 1.9† (n = 7)
τ of inactivation at +20 mV (τ_{inact} in ms)	47.3 ± 2.0 (n = 15)	87.2 ± 6.2* (n = 15)	47.5 ± 2.2 (n = 15)	66.6 ± 3.5† (n = 15)
Time to peak at +50 mV (TtP in ms)	4.5 ± 0.2 (n = 20)	14.4 ± 1.4* (n = 16)	4.1 ± 0.2 (n = 15)	6.1 ± 0.5† (n = 21)
τ of recovery from inactivation (ms)	419.6 ± 18.8 (n = 6)	485.6 ± 74.8 (n = 6)	89.2 ± 5.3 (n = 6)	60.2 ± 6.9† (n = 6)

*Significantly different from Kv4.3.
†Significantly different from Kv4.3 + KChIP2b.

KCNE2 1.5 μg) using Lipofectamine (Invitrogen Life Technologies, Carlsbad, CA, USA) according to the manufacturer's instructions. In one set of experiments, we also co-transfected equimolar levels of KChIP2b (*KCND3* 1.5 μg, *KCNE2* 1.5 μg, *KCNIP2* 1.5 μg). The transfected cells were then cultured in Ham's F-12 medium (Nakalai Tesque, Inc., Kyoto, Japan) supplemented with 10% fetal bovine serum (JRH Biosciences, Inc., Lenexa, KS, USA) and antibiotics (100 international units per milliliter penicillin and 100 μg/mL streptomycin) in a humidified incubator gassed with 5% CO_2 and 95% air at 37°C. The cultures were passaged every 4 to 5 days using a brief trypsin-EDTA treatment. The trypsin-EDTA treated cells were seeded onto glass coverslips in a Petri dish for later patch-clamp experiments.

Electrophysiologic recordings and data analysis

After 48 hours of transfection, a coverslip with cells was transferred to a 0.5-mL bath chamber at 25°C on an inverted microscope stage and perfused at 1 to 2 mL/min with extracellular solution containing the following (in mM): 140 NaCl, 5.4 KCl, 1.8 $CaCl_2$, 0.5 $MgCl_2$, 0.33 NaH_2PO_4, 5.5 glucose, and 5.0 HEPES; pH 7.4 with NaOH. Cells that emitted green fluorescence were chosen for patch-clamp experiments. If co-expressed with *KCNE2* (or its mutants), the cells were incubated with polystyrene microbeads precoated with anti-CD8 antibody (Dynabeads M450, Dynal, Norway) for 15 minutes. In these cases, cells that emitted green fluorescence and had attached beads were chosen for electrophysiologic recording. Whole-cell membrane currents were recorded with an EPC-8 patch-clamp amplifier (HEKA, Lambrecht, Germany), and data were low-pass filtered at 1 kHz, acquired at 5 kHz through an LIH-1600 analog-to-digital converter (HEKA), and stored on hard disk using PulseFit software (HEKA). Patch pipettes were fabricated from borosilicate glass capillaries (Narishige, Tokyo, Japan) using a horizontal microelectrode puller (P-97, Sutter Instruments, Novato, CA, USA) and the pipette tips fire-polished using a microforge. Patch pipettes had a resistance of 2.5 to 5.0 MΩ when filled with the following pipette solution (in mM): 70 potassium aspartate, 50 KCl, 10 KH_2PO_4, 1 $MgSO_4$, 3 Na_2-ATP (Sigma, Japan, Tokyo), 0.1 Li_2-GTP (Roche Diagnostics GmbH, Mannheim, Germany), 5 EGTA, and 5 HEPES (pH 7.2).

Cell membrane capacitance (C_m) was calculated from 5 mV-hyperpolarizing and depolarizing steps (20 ms) applied from a holding potential of −80 mV according to Equation 1[19]:

$$C_m = \tau_c I_0/\Delta V_m(1 - I_\infty/I_0), \quad (1)$$

where τ_c = time constant of capacitance current relaxation, I_0 = initial peak current amplitude, ΔV_m = amplitude of voltage step, and I_∞ = steady-state current value. Whole-cell currents were elicited by a family of depolarizing voltage steps from a holding potential of −80 mV. The difference between the peak current amplitude and the current at the end of a test pulse (1-second duration) was referred to as the transient outward current. To control for cell size variability, currents were expressed as densities (pA/pF).

Steady-state activation curves were obtained by plotting the normalized conductance as a function of peak outward potentials. Steady-state inactivation curves were generated by a standard two-pulse protocol with a conditioning pulse of 500-ms duration and obtained by plotting the normalized current as a function of the test potential. Steady-state inactivation/activation kinetics were fitted to the following Boltzmann equation (Eq. 2):

$$Y(V) = 1/(1 + \exp[(V_{1/2} - V)/k]), \quad (2)$$

where Y = normalized conductance or current, $V_{1/2}$ = potential for half-maximal inactivation or activation, respectively, and k = slope factor.

Data relative to inactivation time constants, time to peak, and mean current levels were obtained by using current data recorded at +50 mV or +20 mV. Recovery from inactivation was assessed by a standard paired-pulse protocol: a 400-ms test pulse to +50 mV (P1) followed by a variable

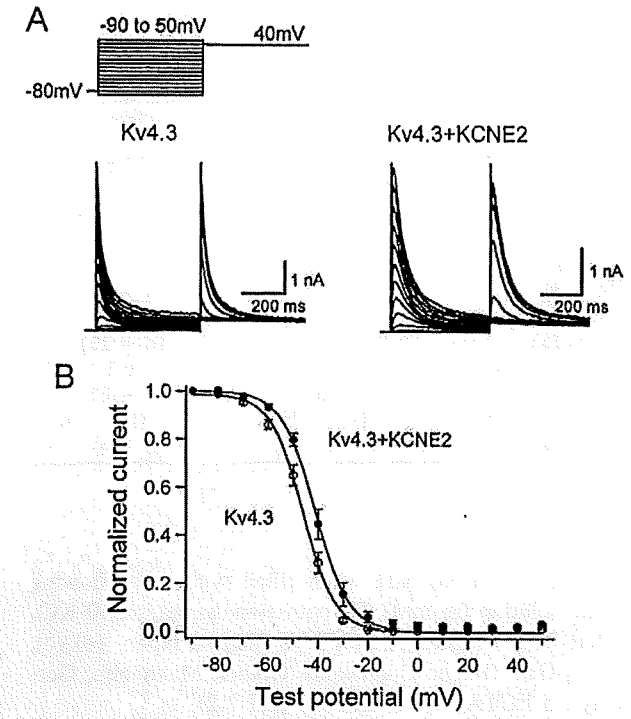

Figure 2 *KCNE2* co-expression with Kv4.3 causes a positive shift of voltage dependence of steady-state inactivation. **A:** Representative Kv4.3 and Kv4.3 + *KCNE2* current traces induced by 500-ms pulses (P1) from −90 to +50 mV applied from the holding potential −80 mV in 10-mV steps followed by a second pulse (P2) to +40 mV. **B:** Steady-state inactivation curves for Kv4.3 *(open circles)* and Kv4.3 + *KCNE2 (closed circles)* channels.

recovery interval at −80 mV and then a second test pulse to +50 mV (P2). Both the inactivation time constants and the time constant for recovery from inactivation were determined by fitting the data to a single exponential (Eq. 3):

$$I(t) \text{ (or } P2/P1) = A + B_{exp}(-t/\tau), \quad (3)$$

where I(t) = current amplitude at time t, A and B = constants, and τ = inactivation time constant or time constant for recovery from inactivation. For measurement of recovery from inactivation, the plot of P2/P1 instead of I(t) was used.

All data were given as mean ± SEM. Statistical comparisons between two groups were analyzed using Student's unpaired t-test. Comparisons among multiple groups were analyzed using analysis of variance followed by Dunnett test. $P < .05$ was considered significant.

Results

Effects of *KCNE2* on Kv4.3 currents and its gating kinetics

WT *KCNE2* initially was co-expressed with *KCND3*, the gene encoding Kv4.3, the α subunit of the I_{to} channel,[17,18] in CHO cells. Figure 1A shows representative whole-cell current traces recorded from cells transfected with *KCND3* and co-transfected with (right) or without (left) *KCNE2*. Cells expressing Kv4.3 channels alone showed rapidly activating and inactivating currents. Co-expression of *KCNE2* significantly reduced peak current densities as summarized in the current–voltage relationship curve shown in Figure 1B and slowed both activation and inactivation kinetics (Table 1). Figure 1C (left) shows mean time intervals from the onset of the pulse to maximum current (time to peak), whereas the right panel shows time constants of inactivation (at +20 mV) obtained using Equation 3. Thus, co-transfection of *KCNE2* significantly increased both the time to peak and the time constant.

In contrast, *KCNE2* did not affect the voltage dependence of steady-state activation as assessed by plotting the normalized conductance as a function of test potential (Figure 1D). Fitting to the Boltzmann equation (Eq. 2) yielded half-maximal activation potentials of −6.5 ± 2.1 mV for Kv4.3 alone (open circles) and −5.5 ± 1.7 mV for Kv4.3 + *KCNE2* channels (filled circles, P = NS; Table 1). These findings are consistent with those previously reported for studies using *Xenopus* oocytes, CHO cells, and HEK293 cells.[20,21]

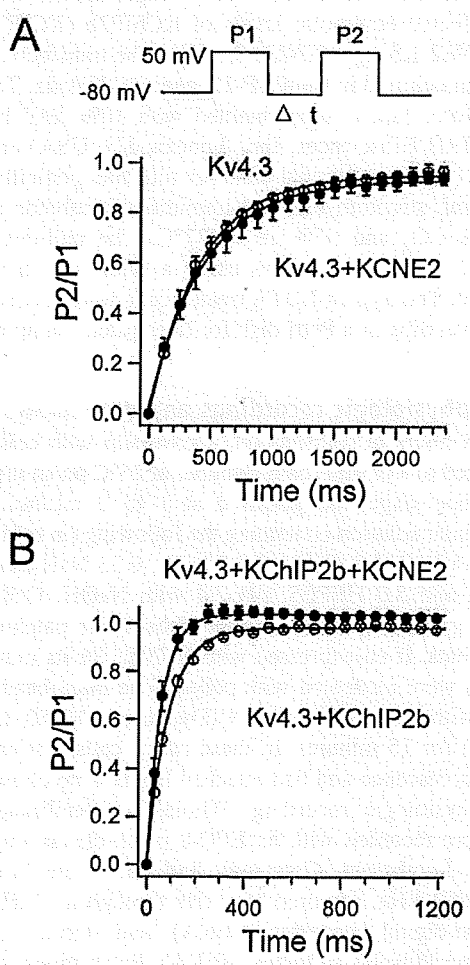

Figure 3 Effects of *KCNE2* co-expression on recovery from inactivation of Kv4.3 (A) and Kv4.3 + KChIP2b (B) currents. Recovery from inactivation was assessed by a two-pulse protocol (A, inset): a 400-ms test pulse to +50 mV (P1) followed by a variable interval at −80 mV, then by a second test pulse to +50 mV (P2). Data were fit to a single exponential.

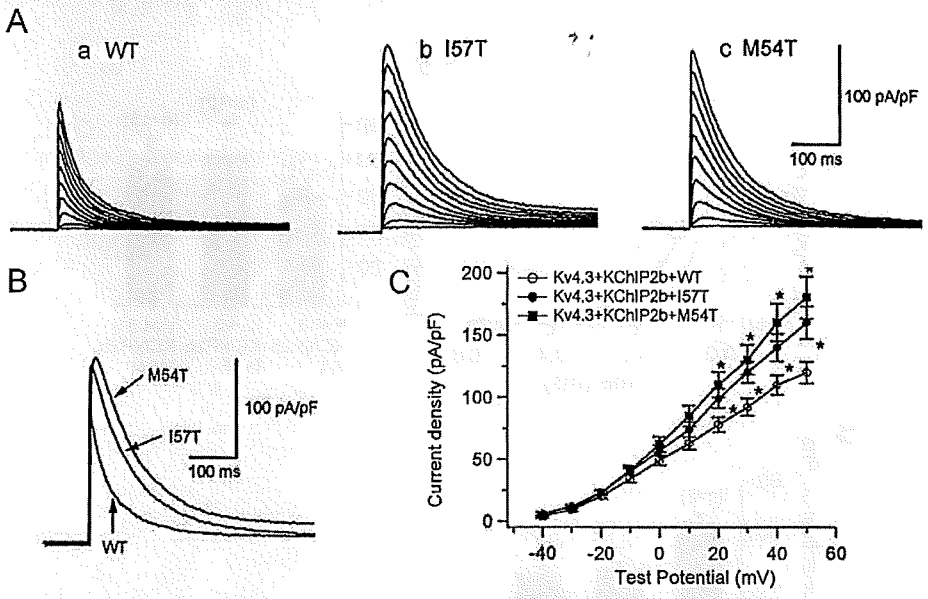

Figure 4 Two *KCNE2* transmembrane variants, I57T and M54T, increase the reconstituted Kv4.3 + KChIP2b channel current and slow its inactivation. **A:** Three sets of current traces elicited by depolarizing pulses for 500 ms from a holding potential of −80 mV to potentials ranging between −40 and +50 mV in 10-mV increments (same protocol as in experiments of Figure 1A). **B:** Superimposition of three original current traces recorded upon depolarization showing variant-related increase in peak outward current density. **C:** Current–voltage relationship curve showing average peak outward current densities (*P <.05 vs Kv4.3 + KChIP2b + WT). WT = wild type.

KCNE2 co-expression also caused a positive shift (approximately +5 mV) of voltage dependence of steady-state inactivation. Steady-state inactivation was assessed using a double-step pulse method (Figure 2A, inset). Peak outward currents recorded at various levels of prepulse (Figure 2A) were normalized by that measured after a 500-ms prepulse at −90 mV and are plotted as a function of prepulse test potentials (Figure 2B). Half-inactivation potentials of steady-state inactivation, determined by fitting data to the Boltzmann equation (Eq. 2), were −46.0 ± 1.3 mV for Kv4.3 (open circles) and −40.8 ± 1.7 mV for Kv4.3 + *KCNE2* (filled circles, P <.01), consistent with the observation of Tseng's group.[13]

A double-pulse protocol (Figure 3A, inset) was used to test the effect of *KCNE2* co-expression on the time course for recovery from inactivation. Figure 3A shows the time course of recovery of Kv4.3 alone (open circles) and Kv4.3 + *KCNE2* (filled circles). Mean time constants for recovery from inactivation were not significantly different, indicating that co-transfection of *KCNE2* did not affect the time course of recovery from inactivation.

Effects of *KCNE2* on Kv4.3 + KChIP2b current and its gating kinetics

For human native cardiac I_{to}, KChIP2 has been shown to serve as a principal β subunit.[22–25] Accordingly, in another series of experiments, we examined the effect of WT and mutant *KCNE2* on Kv4.3 + KChIP2b current. Consistent with previous reports, in the presence of KChIP2, Kv4.3 currents showed a significantly faster recovery from inactivation (Figure 3B and Table 1).[26,27] Co-expression of WT *KCNE2* produced similar changes on Kv4.3 + KChIP2b current as on Kv4.3 current (Table 1). Kv4.3 + KChIP2b current recovery from inactivation was further accelerated: average time constant was 89.2 ± 6.5 ms for Kv4.3 + KChIP2b alone (open circles) and 60.2 ± 8.4 ms for Kv4.3 + KChIP2b + *KCNE2* (filled circles, P <.05). In 16 of 21 cells transfected with *KCNE2*, we observed an "overshoot" phenomenon, which is commonly seen during recording of native I_{to} in human ventricular myocytes.[28]

KCNE2 variants increase Kv4.3 + KChIP2b current and alter its gating kinetics

The I57T variant was first identified in an asymptomatic middle-aged woman with very mild QT prolongation.[6] In addition to this variant, the authors reported another *KCNE2* variant of the transmembrane segment (M54T) that was associated with ventricular fibrillation during exercise in a middle-aged woman. This patient appeared to show a wide range of QTc interval (390–500 ms). Therefore, we tested the functional effects of these two transmembrane *KCNE2* variants on Kv4.3 + KChIP2b currents.

The three panels of Figure 4A show three sets of current traces elicited by depolarizing pulses from a holding potential of −80 mV in cells co-transfected with WT (a), I57T (b), or M54T (c) *KCNE2*. Neither variant caused a significant shift of half-maximal activation voltage: −7.4 ± 1.4 mV (n = 8) for co-expression of WT *KCNE2*, −6.1 ± 1.5 mV (n = 8) for I57T, and −6.6 ± 1.6 mV (n = 8) for M54T. Both variants significantly increased I_{to} density: 125.0 ± 10.6 pA/pF in WT *KCNE2* (n = 21), 178.1 ± 12.1 pA/pF with I57T (n = 9), and 184.3 ± 27.9 pA/pF with M54T (n = 9, Figure 4C).

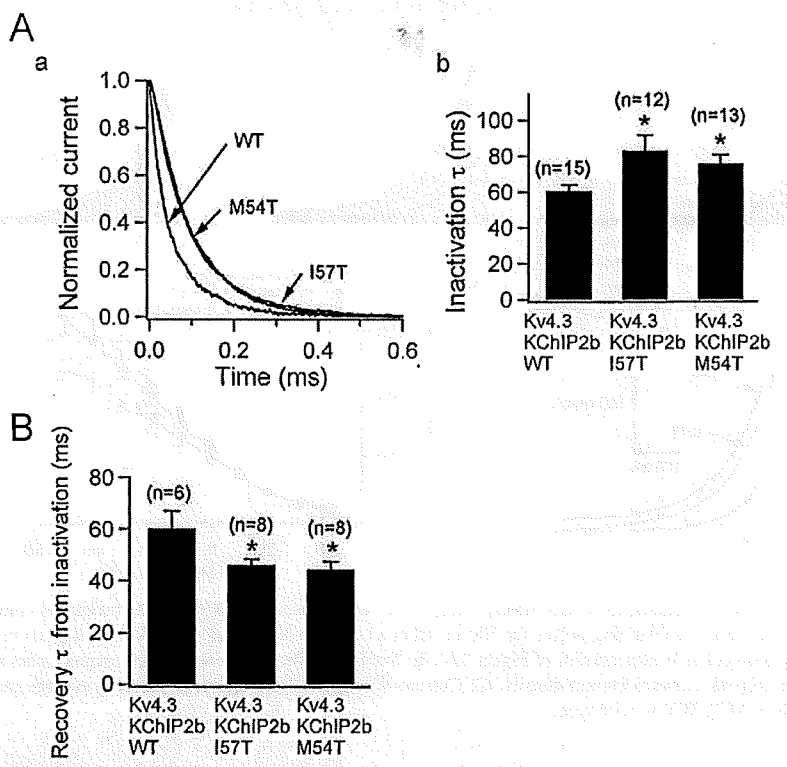

Figure 5 Two *KCNE2* variants slow inactivation kinetics and accelerate recovery from inactivation. **A, a:** Three current traces obtained from Chinese hamster ovary (CHO) cells transfected with wild-type (WT), I57T, and M54T *KCNE2* variant co-expressed with Kv4.3 and KChIP2b. Traces, which are normalized and superimposed, show that the variants slow inactivation. **A, b:** Time constants of decay at +20 mV for WT and variant *KCNE2* (*P <.05 vs Kv4.3 + KChIP2b + WT). Numbers in parentheses indicate numbers of observations. **B:** Time constants of recovery from inactivation recorded using a double-pulse protocol (*P <.05 vs Kv4.3 + KChIP2b + WT). Numbers in parentheses indicate numbers of observations.

Figure 5A shows the three traces depicted in Figure 4B normalized to their peak current level. This representation shows that the time course of inactivation of the two variant currents is slowed. The current decay was fitted by Equation 3 and the time constants (at +20 mV) summarized in Figure 5A, panel b. Finally, Figure 5B shows that the time constants of recovery of the two mutant channels from inactivation were significantly reduced. Thus, compared to WT *KCNE2*, recovery of reconstituted Kv4.3 + KChIP2b channels from inactivation was significantly accelerated with both I57T and M54T mutants.

Discussion

Kv4.3/KChIP2/MiRP1 complex can recapitulate the native I_{to}

In the present study, co-expression of WT *KCNE2* produced changes in kinetic properties (Figures 1–3 and Table 1) that led to close recapitulation of native cardiac I_{to}.[28,29] Notably, in addition to causing a positive shift of steady-state inactivation (Figure 2), *KCNE2* co-expression hastened the recovery of Kv4.3 + KChIP2b channels from inactivation (Figure 3). These modifications rendered Kv4.3 + KChIP2b channels more similar to native cardiac I_{to}, suggesting that *KCNE2* may be an important component of the native I_{to} channel complex. In contrast to a previous observation in HEK293 cells,[21] *KCNE2* co-expression decreased the current density of Kv4.3 and Kv4.3 + KChIP2b channel current in the present study, which seems to be a more reasonable result as the native I_{to} density reportedly was smaller in isolated human heart.[28] *KCNE2* co-expression has also been shown to reduce the density of Kv7.1[8,9] and HERG[6,7] channels.

Similar to the result of Deschenes and Tomaselli,[21] we failed to observe an overshoot during recovery from inactivation when *KCNE2* was co-expressed with Kv4.3 (Figure 3A), which is in contrast to the report of another group.[13] However, co-expression of *KCNE2* with Kv4.3 + KChIP2 channels produced an overshoot (Figure 3B), consistent with the report of Wettwer's group.[25] Wettwer et al also found that other *KCNE* subunits either were ineffective or induced only a small overshoot in CHO cells. Therefore, both MiRP1 and KChIP2 subunits are sufficient and necessary to recapitulate native I_{to} in the heart. Considering that the overshoot phenomenon has been described only in human ventricular I_{to} channels of the epicardial but not endocardial region,[28] these results may further implicate participation of MiRP1 and KChIP2 in the I_{to} channel complex in epicardium.

KCNE2 variants may alter the arrhythmogenic substrate by modulating I_{to}

Heterologous expression in CHO cells was conducted to examine the functional effects of I57T and M54T variants on Kv4.3 + KChIP2 channels. Both I57T and M54T

KCNE2 variants significantly (1) increased peak transient outward current density (Figure 4), (2) slowed the decay of the reconstituted I_{to} (Figure 5A), and (3) accelerated its recovery from inactivation (Figure 5B). Both variants thus caused an important gain of function in human I_{to}. These sequence changes may play a role in modulating I_{to} and thereby predispose to some inherited fatal rhythm disorders.

Functional effects on I_{to} induced by I57T and M54T resemble each other, increasing I_{to} density and accelerating its recovery from inactivation. The gain of function in I_{to} opposes the fast inward Na^+ currents during phase 0 of the action potential, leading to all or none repolarization at the end of phase 1 and loss of the epicardial action potential dome, thus promoting phase 2 reentry and fatal ventricular arrhythmias.[30]

Another *KCNE2* variant (M54T) associated with fatal arrhythmias was first identified in a woman who had a history of ventricular fibrillation and varied QT intervals.[6] It is possible that her arrhythmia was also related to a gain of function in I_{to} secondary to this variation in *KCNE2*. Interestingly, the I57T variant has been reported to produce a loss of function of HERG or Kv7.1 channels, thereby predisposing to long QT syndrome,[6,8] indicating that the same *KCNE2* variant could cause two different cardiac rhythm disorders, similar to long QT syndrome and Brugada syndrome caused by *SCN5A* mutations.[31,32]

References

1. Kass RS, Freeman LC. Potassium channels in the heart: cellular, molecular, and clinical implications. Trends Cardiovasc Med 1993;3:149–159.
2. MacKinnon R. Determination of the subunit stoichiometry of a voltage-activated potassium channel. Nature 1991;350:232–235.
3. Abbott GW, Goldstein SA. A superfamily of small potassium channel subunits: form and function of the MinK-related peptides (MiRPs). Q Rev Biophys 1998;31:357–398.
4. Barhanin J, Lesage F, Guillemare E, Fink M, Lazdunski M, Romey G. KvLQT1 and IsK (minK) proteins associate to form the I_{Ks} cardiac potassium current. Nature 1996;384:78–80.
5. Sanguinetti MC, Curran ME, Zou AR, et al. Coassembly of KvLQT1 and minK (I_{Ks}) proteins to form cardiac I_{Ks} potassium channel. Nature 1996; 384:80–83.
6. Abbott GW, Sesti F, Splawski I, et al. MiRP1 forms I_{Kr} potassium channels with HERG and is associated with cardiac arrhythmia. Cell 1999;97:175–187.
7. Sesti F, Abbott GW, Wei J, et al. A common polymorphism associated with antibiotic-induced cardiac arrhythmia. Proc Natl Acad Sci U S A 2000;97: 10613–10618.
8. Tinel N, Diochot S, Borsotto M, Lazdunski M, Barhanin J. *KCNE2* confers background current characteristics to the cardiac KCNQ1 potassium channel. EMBO J 2000;19:6326–6330.
9. Wu DM, Jiang M, Zhang M, Liu XS, Korolkova YV, Tseng GN. *KCNE2* is colocalized with KCNQ1 and *KCNE1* in cardiac myocytes and may function as a negative modulator of $I_{(Ks)}$ current amplitude in the heart. Heart Rhythm 2006;3:1469–1480.
10. Toyoda F, Ueyama H, Ding WG, Matsuura H. Modulation of functional properties of KCNQ1 channel by association of KCNE1 and KCNE2. Biochem Biophys Res Commun 2006;344:814–820.
11. Yu H, Wu J, Potapova I, et al. MinK-related peptide 1: a beta subunit for the HCN ion channel subunit family enhances expression and speeds activation. Circ Res 2001;88:E84–E87.
12. McCrossan ZA, Roepke TK, Lewis A, Panaghie G, Abbott GW. Regulation of the Kv2.1 potassium channel by MinK and MiRP1. J Membr Biol 2009;228:1–14.
13. Zhang M, Jiang M, Tseng GN. MinK-related peptide 1 associates with Kv4.2 and modulates its gating function: potential role as beta subunit of cardiac transient outward channel? Circ Res 2001;88:1012–1019.
14. Delpon E, Cordeiro JM, Nunez L, et al. Functional effects of KCNE3 mutation and its role in the development of Brugada syndrome. Circ Arrhythm Electrophysiol 2008;1:209–218.
15. Roepke TK, Kontogeorgis A, Ovanez C, et al. Targeted deletion of *KCNE2* impairs ventricular repolarization via disruption of $I_{K,slow1}$ and $I_{to,f}$. FASEB J 2008;22:3648–3660.
16. Calloe K, Cordeiro JM, Di Diego JM, et al. A transient outward potassium current activator recapitulates the electrocardiographic manifestations of Brugada syndrome. Cardiovasc Res 2009;81:686–694.
17. Dixon JE, Shi W, Wang HS, et al. Role of the Kv4.3 K^+ channel in ventricular muscle. A molecular correlate for the transient outward current. Circ Res 1996;79:659–668.
18. Kääb S, Dixon J, Duc J, et al. Molecular basis of transient outward potassium current downregulation in human heart failure: a decrease in Kv4.3 mRNA correlates with a reduction in current density. Circulation 1998;98:1383–1393.
19. Benitah JP, Gomez AM, Bailly P, et al. Heterogeneity of the early outward current in ventricular cells isolated from normal and hypertrophied rat hearts. J Physiol 1993;469:111–138.
20. Singleton CB, Valenzuela SM, Walker BD, et al. Blockade by N-3 polyunsaturated fatty acid of the Kv4.3 current stably expressed in Chinese hamster ovary cells. Br J Pharmacol 1999;127:941–948.
21. Deschênes I, Tomaselli GF. Modulation of Kv4.3 current by accessory subunits. FEBS Lett 2002;528:183–188.
22. Wang S, Bondarenko VE, Qu Y, Morales MJ, Rasmusson RL, Strauss HC. Activation properties of Kv4.3 channels: time, voltage and $[K^+]_o$ dependence. J Physiol 2004;557:705–717.
23. An WF, Bowlby MR, Betty M, et al. Modulation of A-type potassium channels by a family of calcium sensors. Nature 2000;403:553–556.
24. Decher N, Uyguner O, Scherer CR, et al. hKChIP2b is a functional modifier of hKv4.3 potassium channels: cloning and expression of a short hKChIP2b splice variant. Cardiovasc Res 2001;52:255–264.
25. Radicke S, Cotella D, Graf EM, et al. Functional modulation of the transient outward current I_{to} by *KCNE* beta-subunits and regional distribution in human non-failing and failing hearts. Cardiovasc Res 2006;1:695–703.
26. Deschênes I, DiSilvestre D, Juang GJ, Wu RC, An WF, Tomaselli GF. Regulation of Kv4.3 current by KChIP2b splice variants: a component of native cardiac I_{to}? Circulation 2002;106:423–429.
27. Radicke R, Vaquero M, Caballero R, et al. Effects of MiRP1 and DPP6 β-subunits on the blockade induced by flecainide of Kv4.3/KChIP2 channels. Br J Pharmacol 2008;154:774–786.
28. Wettwer E, Amos GJ, Posival H, Ravens U. Transient outward current in human ventricular myocytes of subepicardial and subendocardial origin. Circ Res 1994; 75:473–482.
29. Patel SP, Campbell DL. Transient outward potassium current, "I_{to}," phenotypes in the mammalian left ventricle: underlying molecular, cellular and biophysical mechanisms. J Physiol 2005;569:7–39.
30. Antzelevitch C. Brugada syndrome. Pacing Clin Electrophysiol 2006;29:1130–1159.
31. Bezzina C, Veldkamp MW, van den Berg MP, et al. A single Na^+ channel mutation causing both long-QT and Brugada syndromes. Circ Res 1999;85: 1206–1213.
32. Van den Berg MP, Wilde AA, Viersma TJW, et al. Possible bradycardic mode of death and successful pacemaker treatment in a large family with features of long QT syndrome type 3 and Brugada syndrome. J Cardiovasc Electrophysiol 2001;12:630–636.

Circulation Journal
Official Journal of the Japanese Circulation Society
http://www.j-circ.or.jp

ORIGINAL ARTICLE
Arrhythmia/Electrophysiology

Comparison of Antiarrhythmics Used in Patients With Paroxysmal Atrial Fibrillation:

Subanalysis of J-RHYTHM Study

Yoshiyasu Aizawa, MD; Shun Kohsaka, MD; Shinya Suzuki, MD*; Hirotsugu Atarashi, MD**; Shiro Kamakura, MD†; Masayuki Sakurai, MD††; Haruaki Nakaya, MD‡; Masahiko Fukatani, MD‡‡; Hideo Mitamura, MD§; Tsutomu Yamazaki, MD*; Takeshi Yamashita, MD§§; Satoshi Ogawa, MD; J-RHYTHM Investigators

Background: The J-RHYTHM (Japanese Rhythm Management Trial for Atrial Fibrillation) study demonstrated the benefit of rhythm-control compared with rate-control in Japanese patients with paroxysmal atrial fibrillation (AF), according to AF-specific quality of life scores. However, detailed information on prescribed antiarrhythmic agents remains unclear.

Methods and Results: Data for 419 patients enrolled in the rhythm-control arm of J-RHYTHM were analyzed. The primary endpoint was defined as a composite of total mortality, cerebral infarction, embolism, bleeding, heart failure, and physical/psychological disability. The secondary endpoint was recurrence of AF. The clinical outcome according to choice of initial antiarrhythmic agent (AA) was assessed by Kaplan-Meier survival curve, and further adjusted by Cox-regression hazard model. The primary endpoint occurred in 16.9%, 6.7%, 15.8% and 23.3% of patients assigned to class Ia, Ib, Ic and III agents (P=0.359). The rate of AF recurrence was significantly higher in patients taking a class III drug (Ia, Ib, Ic, III=20.3, 23.3, 29.1, 50.0%; P=0.002). However, after adjustment for other clinical variables, the choice of AA was not associated with recurrence of AF (class I vs III, P=0.15).

Conclusions: The incidence of each endpoint did not differ according to the choice of AA. The class III drugs seemed to lower the sinus rhythm maintenance rate, which might be confounded by other comorbid conditions. (*Circ J* 2010; **74:** 71–76)

Key Words: Antiarrhythmic drugs; Atrial fibrillation; Rhythm control

Atrial fibrillation (AF) is the most common sustained cardiac arrhythmia, and is associated with increased mortality and morbidity.[1–4] Large clinical trials, such as the PIAF (Pharmacological Intervention in Atrial Fibrillation),[5] AFFIRM (Atrial Fibrillation Follow-up Investigation of Rhythm Management),[6] RACE (Rate Control versus Electrical Cardioversion for Persistent Atrial Fibrillation)[7] and STAF (Strategies of Treatment of Atrial Fibrillation)[8] trials, have been conducted to investigate whether rate control or rhythm control improves the outcome of AF, but none of them demonstrated the superiority in the long term of the rhythm control group compared with the rate control group.[5–9]

Recently, the J-RHYTHM (Japanese Rhythm Management Trial for Atrial Fibrillation), the first randomized comparison ever conducted in Japan, demonstrated that compared with the rate-control strategy the rhythm-control strategy was associated with fewer primary endpoints when it included patients' tolerability.[10] Moreover, the AF specific quality of life score was significantly higher in the rhythm-control group. Notably, the study population in the J-RHYTHM study comprised relatively young and predominantly symptomatic patients with PAF rather than persistent AF, when compared with the previous clinical trials.

However, detailed information about each antiarrhythmic agent (AA) has not been provided. In the J-RHYTHM study,

Received May 21, 2009; revised manuscript received September 7, 2009; accepted September 13, 2009; released online December 2, 2009 Time for primary review: 18 days

Keio University School of Medicine, *University of Tokyo, **Nippon Medical School, Tokyo, †National Cardiovascular Center, Suita, ††Hokko Memorial Hospital, Sapporo, ‡Chiba University, Chiba, ‡‡Chikamori Hospital, Kochi, §Saiseikai Central Hospital and §§Cardiovascular Institute, Tokyo, Japan

Mailing address: Yoshiyasu Aizawa, MD, Division of Cardiology, Department of Internal Medicine, Keio University School of Medicine, 35 Shinano-machi, Shinjuku-ku, Tokyo 160-8582, Japan. E-mail: yoshiyaaizawa-circ@umin.ac.jp

ISSN-1346-9843 doi:10.1253/circj.CJ-09-0367

Table 1. Antiarrhythmic Agents Used in the J-RHYTHM Study According to the VW Classification

Class Ia	Cibenzoline
	Disopyramide
	Pirmenol
Class Ib	Aprindine
Class Ic	Pilsicainide
	Propafenone
	Flecainide
Class III	Bepridil
	Amiodarone

J-RHYTHM, Japanese Rhythm Management Trial for Atrial Fibrillation; VW, Vaughan Williams.

AAs were selected by the attending physicians principally based on recommendations from the Japanese Circulation Society (JCS) Guideline for Atrial Fibrillation Management to safely and effectively maintain sinus rhythm in assigned patients.[10–12] This substudy was conducted to examine detailed information about each of the AAs used in the J-RHYTHM study.

Methods

Database of the J-RHYTHM Study

The J-RHYTHM study was a randomized multicenter comparative study of patients with PAF treated by either rate or rhythm control.[10,12] PAF was defined as AF expected to convert spontaneously to sinus rhythm within 48 h of onset. Patients were randomly assigned to either control strategy group and the 419 patients assigned to the rhythm-control group were analyzed in this substudy. The AAs were selected by the attending physicians according to the "JCS Guideline for Atrial Fibrillation Management".[11] In this guideline, a class I drug was the drug of choice for PAF, whereas the ACC/AHA/ESC Guidelines for the Management of Patients With Atrial Fibrillation recommend flecainide, propafenone, or sotalol as the initial drug for recurrent PAF without heart disease.[13]

Oral antithrombotic therapy was applied in the rhythm-control arm according to the protocol modified from the AFFIRM study.[6,14] Briefly, in patients with 1 or more risk factors for stroke, warfarin was prescribed to maintain the prothrombin time–international normalized ratio (PT-INR) between 1.6 and 3.0. Anticoagulant therapy was continued throughout the study, even if sinus rhythm appeared to be maintained by the AAs.[10,12] A total of 38 patients dropped out (6.9%) during the study, we excluded 8 patients with no medication on entry to the study (6 of them were given no drugs during the follow-up period) and 1 patient was being treated by 2-drug combinations on entry to the study.

Classification of Antiarrhythmic Agents

We classified the AAs according to the Vaughan Williams system to compare the incidence of various endpoints in the rhythm-control group of the J-RHYTHM study (Table 1).

Endpoints

We defined the primary endpoint as a combination of hard and soft endpoints. The hard endpoint was a composite of total mortality, symptomatic cerebral infarction, systemic embolism, major bleeding and hospitalization for heart failure requiring intravenous administration of diuretics. The soft endpoint was physical/psychological disability requiring alteration of the assigned treatment strategy.

The secondary endpoint was recurrence of AF during the follow-up period. The maintenance of sinus rhythm was confirmed by snapshot ECG recorded at the outpatient clinic every 3 months.

Statistical Analysis

Baseline clinical characteristics of patients were compared with chi-square tests and 1-way ANOVA. Rates for all time-to-event analyses were estimated by the Kaplan-Meier method[15] and were compared by the log-rank test. Secondary analyses were conducted to evaluate results within subgroups according to prescribed AAs. Unadjusted hazard ratios for the secondary endpoint were estimated by logistic regression analysis. Known clinical predictors, such as age, sex, presence or absence of congestive heart failure, coronary artery disease, valvular heart disease, cardiomyopathy, history of previous medication for AF and Vaughan Williams classification (class I vs class III), were used to construct a multivariable Cox-proportional hazard model by a stepwise procedure. A 2-tailed P value <0.05 was considered statistically significant.

Results

Baseline Patient Characteristics

For the 419 patients with PAF assigned to rhythm control, the median follow-up period was 1.7 years (interquartile

Table 2. Baseline Characteristics of Patients

	Overall (n=381)	Class of AA Ia (n=118)	Ib (n=30)	Ic (n=203)	III (n=30)	P value
Age (years)	65.1±10.1	65.3±10.3	64.7±9.3	65.2±10.0	64.4±11.7	0.96
Male (%)	267 (70.0)	76 (64.4)	21 (70.0)	144 (70.9)	26 (86.7)	0.12
CHF (%)	13 (3.4)	3 (2.5)	1 (3.3)	8 (3.9)	1 (3.3)	0.93
CAD (%)	28 (7.3)	8 (6.8)	3 (10)	15 (7.4)	2 (6.7)	0.94
Valvular disease (%)	20 (5.2)	7 (5.9)	1 (3.3)	10 (4.9)	2 (6.7)	0.91
Cardiomyopathy (%)	6 (1.6)	0 (0)	0 (0)	6 (3.0)	0 (0)	0.14
Duration of PAF (days)	2,642±7,367	1,585±4,974	2,472±6,955	3,362±8,893	2,097±1,911	0.20
History of Rx (%)	135 (35.4)	44 (37.2)	10 (33.3)	65 (32.0)	16 (53.3)	0.14

Data are mean±SD or n (%).
AA, antiarrhythmic agent; CHF, congestive heart failure; CAD, coronary artery disease; PAF, paroxysmal atrial fibrillation; Rx, treatment.

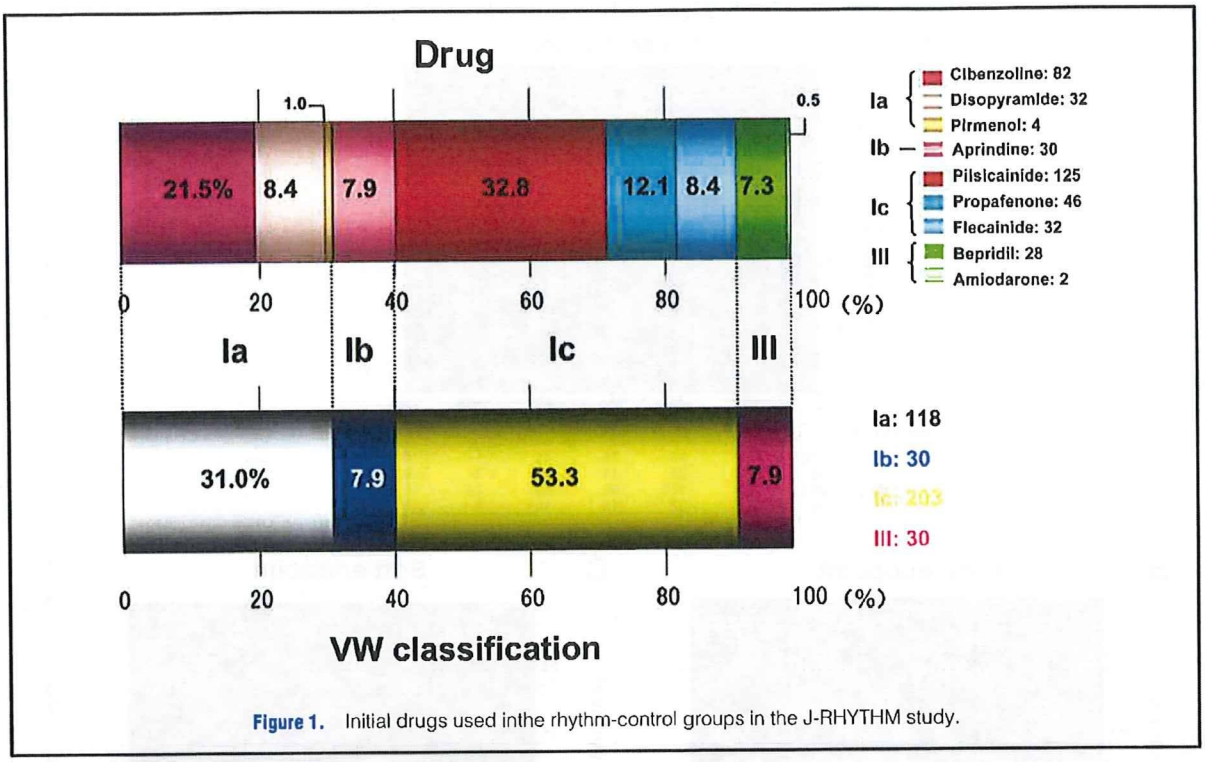

Figure 1. Initial drugs used inthe rhythm-control groups in the J-RHYTHM study.

Table 3. Adverse Events

	Class of AA					P value
	Overall (n=381)	Ia (n=118)	Ib (n=30)	Ic (n=203)	III (n=30)	
Primary endpoint	61 (16.0)	20 (16.9)	2 (6.7)	32 (15.8)	7 (23.3)	0.35
Hard endpoint	18 (4.7)	6 (5.0)	1 (3.3)	9 (4.4)	2 (6.7)	0.92
Total mortality	4 (1.0)	1 (0.8)	0 (0)	2 (1.0)	1 (3.3)	0.59
Symptomatic stroke	9 (2.4)	2 (1.7)	1 (3.3)	6 (3.0)	0 (0)	0.70
Systemic embolism	1 (0.3)	1 (0.8)	0 (0)	0 (0)	0 (0)	0.52
Major bleeding	2 (0.5)	1 (0.8)	0 (0)	0 (0)	1 (3.3)	0.11
Heart failure	2 (0.5)	1 (0.8)	0 (0)	1 (0.5)	0 (0)	0.90
Soft endpoint						
QOL decrease	43 (11.3)	14 (11.2)	1 (3.3)	23 (11.3)	5 (16.7)	0.42

Data are n (%). AA, antiarrhythmic agent.

range: 0.85–2.4 years), the mean age was 65.1±10.1 years, 70.0% were men, 3.4% had a history of congestive heart failure, 7.3% had coronary artery disease, 5.2% had valvular heart disease, 1.6% had cardiomyopathy, the mean duration after onset of PAF was 7.2±20 years, and 35.4% had a history of prior medical treatment for PAF (Table 2). These patients' clinical characteristics were not different among users of each AA classified by the Vaughan Williams classification.

Treatment

AAs prescribed at the beginning of study are outlined in Figure 1. The AAs used in the rhythm-control group were different from those used in previous clinical trials.[5-8] Approximately 80% of patients were started on class Ia or Ic drugs in accordance with the "The JCS Guideline for Atrial Fibrillation Management".[11] In addition, bepridil was the class III drug used in 7.3% of cases, and amiodarone was prescribed in only 0.5% of the patients as an initial therapy. Anticoagulation with warfarin was performed in 60% of the patients appropriately, according to CHADS2 risk assessment.[10]

Primary Endpoint

The primary endpoint occurred in 20 (16.9), 2 (6.7), 32 (15.8) and 7 (23.3) patients (%) assigned to class Ia, Ib, Ic or III drugs, respectively. Details of events defined as the primary endpoint are outlined in Table 3. The total mortality was 4 (1%) and did not differ significantly among the AA groups. Kaplan-Meier estimates of the first occurrence of the primary endpoint over time are shown in Figure 2A. The occurrence of the primary endpoint was not significantly different among the drug groups. A similar trend was seen

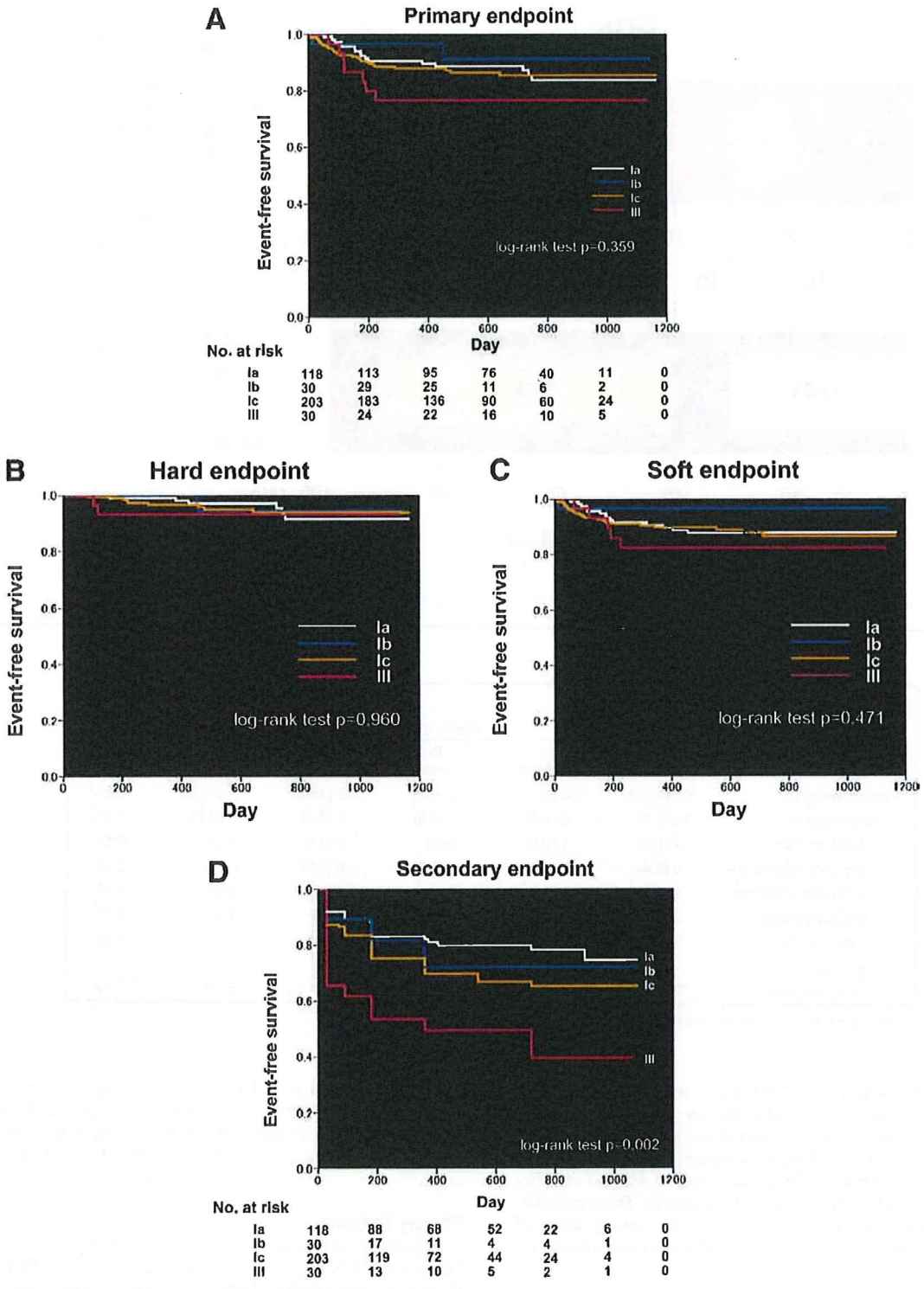

Figure 2. (**A**) Kaplan-Meier curve for event-free survival (primary endpoint = hard and soft endpoints). (**B**) Event-free survival curves for hard endpoints: total mortality, symptomatic cerebral infarction, systemic embolism, major bleeding and hospitalization for heart failure requiring intravenous administration of diuretics. (**C**) Event-free survival curves for soft endpoint (physical/psychological disability requiring alteration of the assigned treatment strategy). (**D**) Kaplan-Meier curve for event-free survival (secondary endpoint).

when hard and soft endpoints were analyzed separately (Figures 2B,C).

Secondary Endpoint

Sinus Rhythm Maintenance AF documented by snapshot ECG during follow-up occurred in 20.3, 23.3, 29.1, 50.0% of the patients assigned to class Ia, Ib, Ic or III drugs, respectively. Kaplan-Meier estimates of the first occurrence of the secondary endpoint over time are shown in Figure 2D. The recurrence of AF was significantly higher in patients treated with class III drugs (P=0.002).

Hazard Ratios in Subgroups We created a multivariable Cox proportional hazard model by stepwise procedure to exclude confounding factors. After adjustment for other clinical variables, the choice of AA was no longer associated with recurrence of AF (class I vs III, P=0.15). Hazard ratios for the secondary endpoint in the subgroups are shown in Table 4. Presence of cardiomyopathy and history of previous rhythm control therapy were associated with the occurrence of the secondary endpoint, but the difference between class I and class III drugs was not associated with the difference in AF-free survival rate. Additionally, this trend did not alter when we excluded 6 patients with cardiomyopathy.

Table 4. Cox Proportional Hazard Model

	Hazard ratio	95%CI	P value
Age	0.988	0.32–1.65	0.21
Sex	1.207	0.77–1.64	0.38
CHF	1.542	0.54–2.55	0.38
CAD	0.995	0.20–1.79	0.99
Valvular disease	0.972	0.11–1.84	0.94
Cardiomyopathy	3.954	3.00–4.91	0.004
History of Rx	1.628	1.24–2.01	0.012
VW classification (I vs III)	1.214	0.98–1.45	0.15

CI, confidence of interval. Other abbreviations see in Tables 1,2.

Discussion

Main Results

The incidence of the primary endpoint did not differ significantly between each group of AAs classified by the Vaughan Williams classification. The rhythm maintenance rate seemed to be lower with class III agents, but this effect was not independent after adjustment for other comorbidities of the patients.

The patients in the J-RHYTHM study were characterized by PAF, young age, less structural heart disease, and less previous history of congestive heart failure, predicting good prognosis. Only ~20% of patients were at high risk for stroke. Thus, the total mortality and cardiovascular morbidity rates were low compared with previous studies, in which most or all of the patients had persistent AF and were treated by amiodarone.[5–8] The AAs used in the present rhythm-control group were also different from those used in previous studies,[5–8,10,12] in which physicians selected the drugs principally according to the "The Japanese Guideline for Atrial Fibrillation Management".[11] In the present study, a total of 30.2% patients were started on class Ia drugs, 7.7% on Ib drugs, 52.0% on Ic drugs, and 7.7% on III drugs (7.3% of bepridil and 0.5% of amiodarone). Bepridil, a multichannel blocker, is a reverse remodeling agent that has had its efficacy established by several studies conducted in Japan.[16–21]

The present study shows that in the rhythm-control group, the hard and soft endpoints were not affected by the selection of AA. Regarding the long-term safety of class III agents, there was 1 death during the follow-up period. Because our analysis did not have a control group for reference, we were unable to draw a definite conclusion about the use of bepridil. The recently published J-BAF study also demonstrated drug-related adverse effects that suggest caution about using bepridil.[20]

The maintenance of sinus rhythm was significantly decreased with class III drugs. However, the multivariate Cox proportional hazards survival model revealed that maintenance of sinus rhythm was influenced by several factors, such as presence of cardiomyopathy and prior medical treatment for AF, which seems reasonable because rhythm-control therapy is known to be difficult in patients with structural heart disease such as hypertrophic cardiomyopathy. Although these independent factors were not associated with the patients taking class III drugs, involvement of some unidentified underlying factors can not be denied because of the relatively small number of patients in this group of AAs.

Although amiodarone is considered the final choice for PAF patients in Japan, because of its serious side-effect, there is certain evidence that amiodarone prevents AF recurrence in patients with structural heart disease.[5,6,22,23] Therefore, further analysis should be performed to confirm the effect of amiodarone vs bepridil in Japanese patients with PAF.

Another insight gained from this subanalysis regards aprindine, a class Ib drug that was eliminated from the list of first-choice drugs for lone AF in the new "Guidelines of Pharmacotherapy of Atrial Fibrillation (JCS 2008)". However, our analysis shows that oral aprindine has similar efficacy to class Ia and Ic drugs, which could not be presented before publication of the guideline. The elimination of the drug from the new guideline was primarily based on a discussion among members about the frequency of aprindine usage in the J-RHYTHM study and a previous randomized trial demonstrating no beneficial effect of the drug over digoxin.[24]

Study Limitations

We initially tried to compare each AA, but because the number of patients in each AA group was limited, we classified the drugs by the Vaughan Williams classification, which is not based on their activity against cardiac ion channels or arrhythmogenic mechanisms. The Sicilian Gambit classification[25] would be more suitable for addressing the issue, but is difficult for actual analysis. Furthermore, the choice of the AAs used in the J-RHYTHM study was not blinded to physicians and patients, which could lead to biases in the occurrence of endpoints and AF recurrence. Although we attempted to adjust for known clinical varieties, unidentified confounders could have affected the outcome.

Second, although it is a standard method of assessing maintenance of sinus rhythm,[5–8,16–19,22,23] snapshot ECGs may underestimate the recurrence of asymptomatic AF.

Conclusion

Our subanalysis of the J-RHYTHM study demonstrated that the incidence of a primary endpoint did not differ between each group of drugs classified by the Vaughan Williams classification. However, the recurrence of AF was high in patients given class III drugs, which may have resulted from some unknown confounding factors.

Acknowledgments

We thank Ms Junko Ueda for her assistance in preparing the data.

References

1. Benjamin EJ, Wolf PA, D'Agostino RB, Silbershatz H, Kannel WB, Levy D. Impact of atrial fibrillation on the risk of death: The Framingham Heart Study. *Circulation* 1998; **98:** 946–952.
2. Vidaillet H, Granada JF, Chyou PH, Maassen K, Ortiz M, Pulido JN, et al. A population-based study of mortality among patients with atrial fibrillation or flutter. *Am J Med* 2002; **113:** 365–370.
3. Krahn AD, Manfreda J, Tate RB, Mathewson FA, Cuddy TE. The natural history of atrial fibrillation: Incidence, risk factors, and prognosis in the Manitoba Follow-Up Study. *Am J Med* 1995; **98:** 476–484.
4. Suzuki S, Yamashita T, Ohtsuka T, Sagara K, Uejima T, Oikawa Y, et al. Prevalence and prognosis of patients with atrial fibrillation in Japan: A prospective cohort of Shinken Database 2004. *Circ J* 2008; **72:** 914–920.
5. Hohnloser SH, Kuck KH, Lilienthal J. Rhythm or rate control in atrial fibrillation: Pharmacological Intervention in Atrial Fibrillation (PIAF): A randomised trial. *Lancet* 2000; **356:** 1789–1794.
6. Wyse DG, Waldo AL, DiMarco JP, Domanski MJ, Rosenberg Y, Schron EB, et al. A comparison of rate control and rhythm control in patients with atrial fibrillation. *N Engl J Med* 2002; **347:** 1825–1833.
7. Van Gelder IC, Hagens VE, Bosker HA, Kingma JH, Kamp O, Kingma T, et al. A comparison of rate control and rhythm control in patients with recurrent persistent atrial fibrillation. *N Engl J Med* 2002; **347:** 1834–1840.
8. Carlsson J, Miketic S, Windeler J, Cuneo A, Haun S, Micus S, et al. Randomized trial of rate-control versus rhythm-control in persistent atrial fibrillation: The Strategies of Treatment of Atrial Fibrillation (STAF) study. *J Am Coll Cardiol* 2003; **41:** 1690–1696.
9. Steinberg JS, Sadaniantz A, Kron J, Krahn A, Denny DM, Daubert J, et al. Analysis of cause-specific mortality in the Atrial Fibrillation Follow-up Investigation of Rhythm Management (AFFIRM) study. *Circulation* 2004; **109:** 1973–1980.
10. Ogawa S, Yamashita T, Yamazaki T, Aizawa Y, Atarashi H, Inoue H, et al. Optimal treatment strategy for patients with paroxysmal atrial fibrillation: J-RHYTHM Study. *Circ J* 2009; **73:** 242–248.
11. The Japanese Guidelines for Atrial Fibrillation Management. *Jpn Circ J* 2001; **65**(Suppl V): 931–979 (in Japanese).
12. Yamashita T, Ogawa S, Aizawa Y, Atarashi H, Inoue H, Ohe T, et al. Investigation of the optimal treatment strategy for atrial fibrillation in Japan. *Circ J* 2003; **67:** 738–741.
13. Fuster V, Rydén LE, Cannom DS, Crijns HJ, Curtis AB, Ellenbogen KA, et al. ACC/AHA/ESC 2006 Guidelines for the Management of Patients with Atrial Fibrillation: A report of the American College of Cardiology/American Heart Association Task Force on Practice Guidelines and the European Society of Cardiology Committee for Practice Guidelines (Writing Committee to Revise the 2001 Guidelines for the Management of Patients With Atrial Fibrillation): Developed in collaboration with the European Heart Rhythm Association and the Heart Rhythm Society. *Circulation* 2006; **114:** e257–e354.
14. The Planning and Steering Committees of the AFFIRM study for the NHLBI AFFIRM investigators. Atrial fibrillation follow-up investigation of rhythm management: The AFFIRM study design. *Am J Cardiol* 1997; **79:** 1198–1202.
15. Kaplan EL, Meier P. Nonparametric estimation from incomplete observations. *J Am Stat Assoc* 1958; **53:** 457–481.
16. Yasuda M, Nakazato Y, Sasaki A, Kawano Y, Nakazato K, Tokano T, et al. Clinical evaluation of adverse effects during bepridil administration for atrial fibrillation and flutter. *Circ J* 2006; **70:** 662–666.
17. Fujiki A, Sakamoto T, Iwamoto J, Nishida K, Nagasawa H, Mizumaki K, et al. Pharmacological cardioversion of persistent atrial fibrillation with and without a history of drug-resistant paroxysmal atrial fibrillation. *Circ J* 2006; **70:** 1138–1141.
18. Nishida K, Fujiki A, Sakamoto T, Iwamoto J, Mizumaki K, Hashimoto N, et al. Bepridil reverses atrial electrical remodeling and L-type calcium channel downregulation in a canine model of persistent atrial tachycardia. *J Cardiovasc Electrophysiol* 2007; **18:** 765–772.
19. Miyaji K, Tada H, Fukushima Kusano K, Hashimoto T, Kaseno K, Hiramatsu S, et al. Efficacy and safety of the additional bepridil treatment in patients with atrial fibrillation refractory to class I antiarrhythmic drugs. *Circ J* 2007; **71:** 1250–1257.
20. Yamashita T, Ogawa S, Sato T, Aizawa Y, Atarashi H, Fujiki A, et al. Dose-response effects of bepridil in patients with persistent atrial fibrillation monitored with transtelephonic electrocardiograms. *Circ J* 2009; **73:** 1020–1027.
21. Miyaji K, Tada H, Fukushima Kusano K, Hashimoto T, Kaseno K, Hiramatsu S, et al. Efficacy and safety of the additional bepridil treatment in patients with atrial fibrillation refractory to class I antiarrhythmic drugs. *Circ J* 2007; **71:** 1250–1257.
22. Singh BN, Singh SN, Reda DJ, Tang XC, Lopez B, Harris CL, et al. Amiodarone versus sotalol for atrial fibrillation. *N Engl J Med* 2005; **352:** 1861–1872.
23. Roy D, Talajic M, Dorian P, Connolly S, Eisenberg MJ, Green M, et al. Amiodarone to prevent recurrence of atrial fibrillation. *N Engl J Med* 2000; **342:** 913–920.
24. Atarashi H, Inoue H, Fukunami M, Sugi K, Hamada C, Origasa H; Sinus Rhythm Maintenance in Atrial Fibrillation Randomized Trial (SMART) Investigators. Double-blind placebo-controlled trial of aprindine and digoxin for the prevention of symptomatic atrial fibrillation. *Circ J* 2002; **66:** 553–556.
25. Ogawa S. Selection of anti-arrhythmia agents: Application of the Sicilian Gambit. *Nippon Naika Gakkai Zasshi* 1999; **88:** 432–435.

ORIGINAL RESEARCH

Radial Artery Hemodynamic Changes Related to Acupuncture

Shin Takayama, MD,[1] Takashi Seki, MD, PhD,[1#] Norihiro Sugita, Deng,[2] Satoshi Konno, MD, PhD,[3] Hiroyuki Arai, MD, PhD,[3] Yoshifumi Saijo, MD, PhD,[4] Tomoyuki Yambe, MD, PhD,[3] Nobuo Yaegashi, MD, PhD,[1] Makoto Yoshizawa, Deng,[5] and Shin-ichi Nitta, MD, PhD[3]

Background: Assessment of the radial pulse by palpation (pulse diagnosis) is an important diagnostic technique in Traditional Chinese Medicine (TCM), but the changes of blood flow volume in the radial artery during and after acupuncture are unknown.

Objective: The aim of this study was to explore the changes of radial artery blood flow volume during and after acupuncture in healthy subjects.

Design: This study was conducted as a pilot study utilizing a one-group intervention design.

Setting: The study was conducted at a TCM outpatient clinic of Tohoku University Hospital.

Participants: Twenty-six healthy volunteers participated in the study.

Intervention: Acupuncture was performed at LR-3 bilaterally with manual rotation of the needles.

Outcome Measures: Blood pressure was measured at rest and 180 seconds after acupuncture. Radial artery hemodynamics were monitored continuously with a high-resolution ultrasound echo-tracking system. The vessel diameter and blood flow volume of the right radial artery and heart rate were measured at rest, before acupuncture, during acupuncture, and 30, 60, and 180 seconds after acupuncture.

Results: The systolic and diastolic diameter of the radial artery did not significantly change. Radial artery blood flow volume decreased significantly during acupuncture (mean ± SD, 0.16 ± 0.11 mL/sec per m^2; $P < .01$) compared with baseline (0.43 ± 0.27 mL/sec per m^2), but was increased at 180 seconds after acupuncture (0.54 ± 0.28 mL/sec per m^2; $P < .01$).

Conclusions: The present study showed that radial artery blood flow volume decreased immediately during acupuncture at the LR-3 acupoint, but was increased at 180 seconds after acupuncture.

Key words: Acupuncture, radial artery, blood flow volume, ultrasound

(Explore 2010; 6:100-105. © Elsevier Inc. 2010)

INTRODUCTION

Acupuncture is widely used to treat several conditions in Asia and Western countries,[1,2] and it has also been found to be effective for a growing number of other conditions in randomized trials.[3-7] There have been some reports about the hemodynamic effects of acupuncture at a single acupoint,[8-10] but its influence on the changes of blood flow volume in the radial artery has not been discussed.

Acupuncture therapy is adjusted on the traditional diagnostics: looking, listening, smelling, asking, and palpation. Pulse diagnosis at the radial pulse is an important diagnostic technique in Traditional Chinese Medicine (TCM). Although acupuncture has already been shown to influence hemodynamics in the radial artery,[11] no study using a single acupoint has been reported.

In TCM, LR-3 is an acupoint on the Liver meridian, which has the functions of "soothing the Liver" and "regulating the Blood." This point is used in combination with other acupoints for the treatment of hypertension, headache, vertigo, and insomnia.[12]

Recently, some noninvasive methods for measuring peripheral blood flow have been introduced. We employed a new high-resolution echo-tracking system to quantify the continuous changes of radial artery diameter and blood flow volume during acupuncture therapy.

The aim of this study was to clarify the changes of radial artery blood flow volume related to acupuncture.

MATERIALS AND METHODS

Subjects

Twenty-six healthy volunteers who had neither a history of hypertension or hypotension (mean age: 31.7 ± 5.5 years; 21 males and five females) were enrolled. Among them, 11 subjects had previously received acupuncture therapy and 15 had not. This

1 Center for Asian Traditional Medicine, Graduate School of Medicine, Tohoku University, Sendai, Japan
2 Department of Electrical and Communication Engineering, Graduate School of Engineering, Tohoku University, Sendai, Japan
3 Institute of Development, Aging and Cancer, Tohoku University, Sendai, Japan
4 Department of Biomedical Imaging, Graduate School of Biomedical Engineering, Tohoku University, Sendai, Japan
5 Research Division on Advanced Information Technology, Cyberscience Center, Tohoku University, Sendai, Japan
This work was supported by Special Coordination Funds for Promoting Science and Technology from the Japanese Ministry of Education, Culture, Sports, Science and Technology that were awarded to Shin-ichi Nitta
Corresponding Author. Address:
1-1 Seiryo-machi, Aoba-ku, Sendai, Miyagi, Japan
e-mail: t-seki@m.tains.tohoku.ac.jp

ISSN 1550-8307/10/$36.00

doi:10.1016/j.explore.2009.12.001

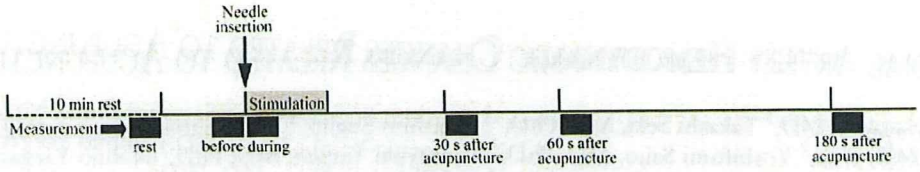

Figure 1. Outline of the test. Acupuncture contains needle insertion and stimulation. *Min,* minutes; *s,* seconds.

study protocol was approved by the Ethics Committee of Tohoku University Graduate School of Medicine and written informed consent to participation was provided by all subjects. After seven subjects were excluded because forearm movements affected the data, 19 were included in the final analysis.

Study Protocol

We performed acupuncture on LR-3 bilaterally and measured the hemodynamics of the radial artery with ultrasound from rest to 180 seconds after acupuncture. The time course of the study is shown in Figure 1.

All investigations were performed under fasting conditions in a quiet, air-conditioned room (constant temperature of 25°C-26°C). Each subject rested in the supine position, and three monitoring electrocardiography electrodes were attached to the chest. Blood pressure was measured with an oscillometer (HEM-9000AI, Omron Healthcare Co Ltd, Kyoto, Japan) on the left arm, and radial artery hemodynamics were assessed with an ultrasound system (Prosoundα10, Aloka Co Ltd, Tokyo, Japan). This system had a high-resolution linear array transducer (13 MHz), and computer-assisted analysis software (e-Tracking system, Aloka Co Ltd) that detected the vessel edge automatically and could measure the vessel diameter and blood flow volume continuously.[13] The right arm was fixed and the right radial artery was scanned longitudinally at 1 to 2 cm above the radial styloid process where the vessel diameter and Doppler wave readings were stable. At the site where the clearest B-mode image of the anterior and posterior intimal interfaces between the lumen and vessel wall was obtained, the transducer was fixed in a special probe holder (MP-PH0001, Aloka Co Ltd; Figure 2), and compression of the artery was carefully avoided. When the tracking gate was placed on the intima, the radial artery diameter was monitored automatically and a waveform of the changes of vessel diameter over the cardiac cycle was displayed in real time by using the e-Tracking system (Figure 3). To obtain accurate measurements, a Doppler angle of 60 degrees or less was maintained.[14,15] Blood flow volume was calculated automatically as the Doppler flow velocity (corrected for the angle) multiplied by the heart rate and the vessel cross-sectional area.[14-16]

After 10 minutes of rest in the supine position, measurement of blood pressure and right radial artery hemodynamics was started.[17,18] Acupuncture was performed by a licensed acupuncturist. A disposable fine stainless steel needle (diameter: 0.16 mm; length: 40 mm; Seirin Co Ltd, Shizuoka, Japan) was inserted at LR-3 bilaterally and maintained at a depth of 10 mm during the test session. LR-3 is located on the foot at 1.5- to 2-finger units above the web between the first and second toes.[15] After the needle was inserted, stimulation (rotating the needles manually bidirectional within an angle of 90 degrees) was performed for 18 seconds.

We measured radial artery hemodynamics after 10 minutes of rest, before acupuncture (=baseline), during acupuncture, and 30 seconds, 60 seconds, and 180 seconds after acupuncture (Figure 1). The hemodynamic parameters, including the radial artery diameter and blood flow volume, and the heart rate, were recorded continuously. To minimize the influence of respiration

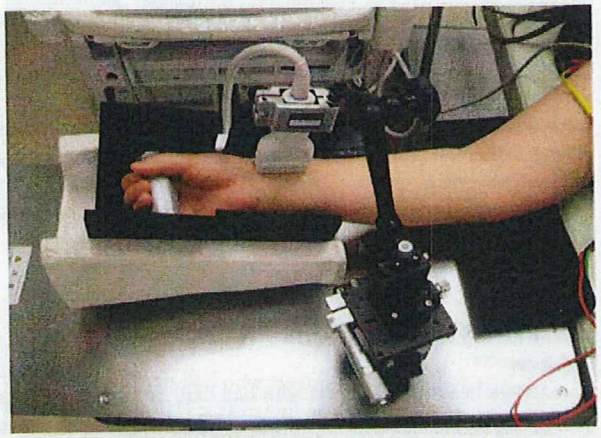

Figure 2. Ultrasound monitoring of radial artery by using a special probe holder.

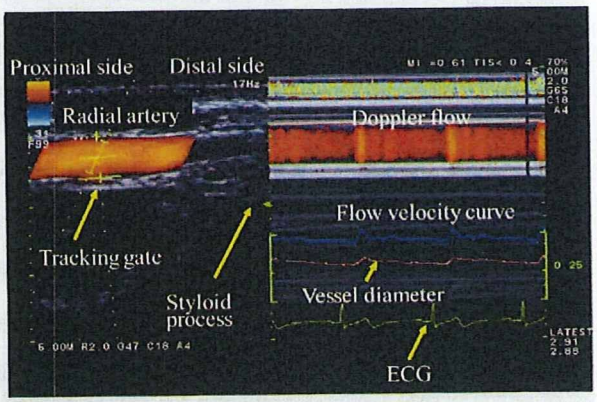

Figure 3. Vessel image and position of the tracking gate (*left*). Changes of radial artery diameter, Doppler flow, and flow velocity (*right*) determined with an automated edge detection device and computer analysis software.

Table 1. Summary of Hemodynamic Parameters. Values are the mean ± SD. AP indicates acupuncture; Syt D, systolic radial artery diameter; Dia D, diastolic radial artery diameter; BFV, radial artery blood flow

	rest	before AP	during AP	30 s after AP	60 s after AP	180 s after AP
Syst D (mm)	2.87 ± 0.46	2.88 ± 0.46	2.84 ± 0.45	2.83 ± 0.45	2.84 ± 0.45	2.88 ± 0.42
Dia D (mm)	2.82 ± 0.46	2.82 ± 0.46	2.79 ± 0.45	2.78 ± 0.44	2.80 ± 0.45	2.84 ± 0.42
BFV (ml/s/m^2)	0.45 ± 0.29	0.43 ± 0.27	0.16 ± 0.11**	0.45 ± 0.30	0.53 ± 0.34*	0.54 ± 0.28**
HR (beats/min)	66.5 ± 9.7	66.6 ± 9.3	60.9 ± 9.1*	64.6 ± 8.4*	64.9 ± 8.0*	65.4 ± 9.0
Syst BP (mmHg)	118.9 ± 12.4	...	...	...	...	116.9 ± 12.9*
Dia BP (mmHg)	69.8 ± 10.1	...	...	...	...	70.5 ± 10.0

on the hemodynamic data, the subjects were asked to breathe every six seconds during the test, and the values of the hemodynamic parameters were averaged for each six-second period. Blood pressure was measured under resting conditions and at 180 seconds after acupuncture.

Statistical Methods

Statistical analysis was performed with SPSS software (version 16.0, SPSS Japan Inc, Tokyo, Japan). Repeated measure analysis of variance, followed by Dunnett's post hoc test, was used for statistical comparison between the measure points. Results are presented as the mean ± SD, and $P < .05$ was taken to indicate significance for all analysis.

RESULTS

We excluded subjects in whom the diameter of the radial artery varied by more than 0.2 mm due to movement of the right forearm during the test from statistical analysis.

Hemodynamic changes, including the radial artery diameter and blood flow volume, the heart rate, and the blood pressure, are summarized in Table 1.

Radial Artery Diameter

The radial artery diameter was measured in millimeters and the percentage of change at each time was calculated in relation to the baseline value. Figure 4A shows the percentage changes of systolic radial artery diameter and Figure 4B shows the percentage changes of diastolic diameter. Both the systolic and diastolic radial artery diameter did not change significantly during the test.

Radial Artery Blood Flow Volume

The blood flow volume was determined as milliliters per second per square meter and then percentage changes were calculated in relation to the baseline value. Figure 4C illustrates the profile of changes in radial artery blood flow volume. There was no significant difference of blood flow volume between that measured after 10 minutes of rest and the baseline value, demonstrating that blood flow volume was stable under resting conditions. The blood flow volume decreased significantly during acupuncture ($P < .01$), but showed a significant increase at both 60 seconds after acupuncture ($P < .05$) and 180 seconds after acupuncture ($P < .01$).

Heart Rate

Heart rate was significantly decreased relative to baseline during acupuncture ($P < .05$), as well as at 30 seconds ($P < .05$) and 60 seconds ($P < .05$) after acupuncture. Heart rate returned to baseline by 180 seconds after acupuncture.

Blood Pressure

Systolic blood pressure showed a significant decrease from the resting value to 180 seconds after acupuncture ($P < .05$), but there was no significant change of diastolic blood pressure.

Side Effects of Acupuncture

No local complications (such as bleeding, hematoma, or infection) occurred.

DISCUSSION

Major Findings

In this study, we used a high-resolution ultrasound echo-tracking system to demonstrate the immediate (during acupuncture) and late (at 180 seconds after acupuncture) changes of radial artery blood flow volume associated with acupuncture at LR-3.

Interpretations

Immediate changes of radial artery blood flow volume. The systolic and diastolic diameter of the radial artery did not significantly change during the test. Thus, an immediate decrease of blood flow volume was observed during acupuncture. The effect of acupuncture on radial artery hemodynamics was presumably due to an increase of sympathetic tone when pain was caused by needle insertion because of extremely rapid response. Elie and Guiheneuc[19] reported that pain stimulation evokes a cutaneous sympathetic response, which appears within 1 to 3 seconds after the stimulus and is of short duration.[20-22] In contrast to other parts of the body, vasomotor regulation and blood flow changes in the hand are entirely regulated by sympathetic nerves.[20,21] Blood flow velocity is mainly influenced by distal resistance, so the marked variability of blood flow patterns is assumed to be related to changes of vasomotor activity. It has been reported that lumbar sympathectomy leads to an increase of forward flow and the disappearance of reverse flow in the femoral artery.[23] Therefore, the immediate response of radial artery blood flow volume to needle insertion was presumably related to an increase of peripheral resistance caused by the vasoconstrictor re-

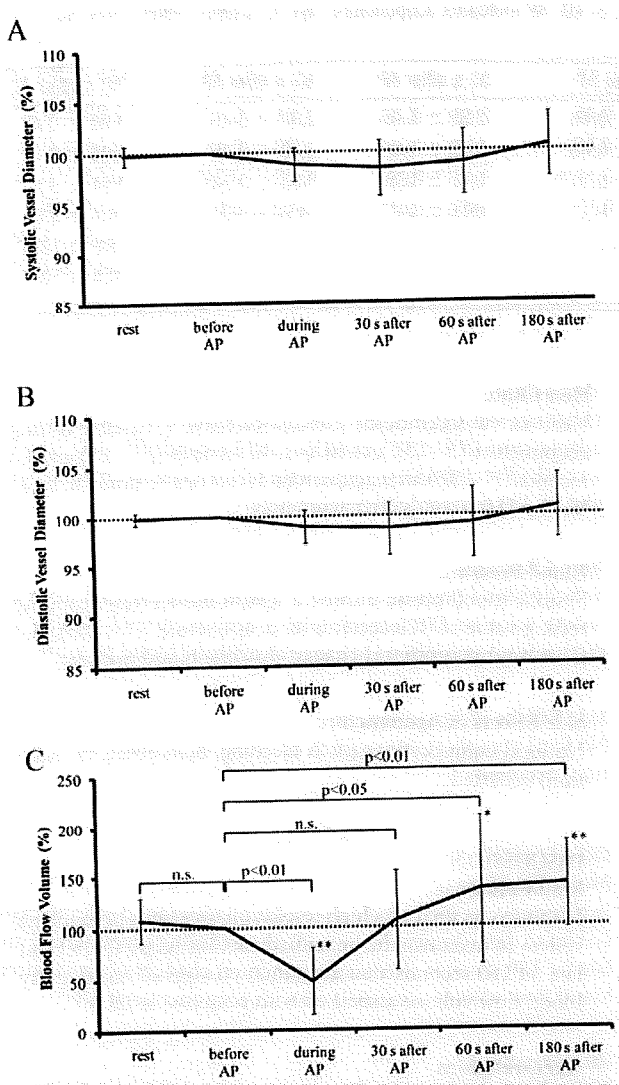

Figure 4. (*A*) Percentage change of systolic radial artery diameter. (*B*) Percentage change of diastolic radial artery diameter. (*C*) Percentage change of radial artery blood flow volume. The percentages of change for each variable are relative to the six-second period before acupuncture. $*P < .05$, $**P < .01$ vs six-second period before acupuncture. *AP*, acupuncture; *s*, second.

sponse to an instantaneous increase of sympathetic tone. If the decrease of blood flow volume was due to increased sympathetic vascular tone, why did the heart rate also decrease during acupuncture? It has been reported that acupuncturelike stimulation of the lower extremity can induce bradycardia via a supraspinal reflex.[24] Thus, it is possible that needle insertion causes a sudden increase of sympathetic tone, after which the supraspinal reflex evoked bradycardia during needle stimulation.

Late changes of radial artery blood flow volume. A late increase of blood flow volume was also observed, along with an increase of the time velocity integral (which is the sum of the velocities), although there was no significant change of vessel diameter. The e-Tracking system cannot simultaneously assess the pulsatility index or resistive index, which are measures of distal vascular resistance. However, continuous recording with this system revealed that the blood flow velocity pattern changed gradually from 60 seconds after acupuncture (data not shown). Diastolic flow velocity increased and the duration of forward flow was longer than before. These changes of the blood flow pattern suggested that the increase of diastolic flow was due to a decrease of distal vascular resistance, which presumably decreased along with peripheral vasodilation secondary to a decrease of vascular tone. Therefore, the late increase of blood flow volume was speculated to indicate a decrease of peripheral vascular tone. There are several reasons why acupuncture might affect peripheral vascular tone. Mechanisms that lead to the inhibition of sympathetic vasoconstriction by acupuncture have been reported.[25] Tsuru and Kawakita[25] have suggested that acupuncture causes vasodilation and increases blood flow in various organs by modulating the central circulatory system and axon reflexes, with the effect depending on the site of stimulation.

Ultrasound measurement. Pulse Doppler sonography is a noninvasive method for assessing blood flow velocity. Blood flow changes rapidly in the arteries of the extremities, especially in the peripheral vessels.[26] Therefore, we measured hemodynamic parameters for 30 seconds after 10 minutes of rest and after obtaining a baseline value to evaluate the stability of resting conditions. It is known that changes of venous return due to respiration cause oscillation of the stroke volume and blood pressure.[27] It can also be inferred from changes of cardiac output that the systemic blood pressure has a similar respiration-related cycle, so the arterial pulse should be modified by breathing.[28] To minimize the influence of respiration on hemodynamics, our subjects were asked to breathe every six seconds during testing and hemodynamic parameters were calculated as average values for each six-second period.

The probe was maintained at the same point throughout the test by using a special holder to ensure that consistent images were obtained. The e-Tracking system automatically measures changes of vessel diameter with a precision of 0.01 mm. Use of this system avoids operator bias, increases reproducibility, and improves accuracy. It was developed for measurement of flow-mediated vasodilatation, which is usually measured at the brachial artery.[17,18] Compared with the brachial artery, the radial artery requires a more sensitive echo-tracking device, although the vessel can be visualized more easily without compression or mechanical distortion. Because the diameter of the radial artery is far smaller than that of the brachial artery, correct assessment of hemodynamics is more difficult and requires some skill. Fixing the probe at the optimal position and avoiding movement of the forearm are both important for obtaining useful data.

Blood pressure. We also demonstrated a decrease of the systemic systolic blood pressure after acupuncture. The mechanism by which acupuncture lowers the blood pressure remains unclear.[29,30] Cardiovascular depression by electroacupuncture in

an animal model has been revealed to be due to stimulation of afferent nerves that triggered an autonomic reflex,[13] whereas an effect on renin secretion has also been reported.[31] In the present study, the systolic blood pressure decreased after acupuncture, but the diastolic blood pressure and heart rate were not significantly changed at 180 seconds after acupuncture. However, the actual changes of these parameters were small, so we would need to investigate more subjects to clarify their significance.

Strengths

We selected the LR-3 acupoint for stimulation in the present study because it is one of the primary acupoints and is used to treat cardiovascular disease in TCM.[12] To the best of our knowledge, the present study is the first to provide physiological evidence that acupuncture at a single acupoint has an effect on radial artery hemodynamics. No previous study using scientific methods has demonstrated such an obvious effect of stimulation at one acupoint. Our findings suggest that acupuncture at a single point can affect sympathetic tone and increase peripheral blood flow, suggesting the need for future studies into the mechanisms underlying such effects.

Limitations

The duration of the test was less than 15 minutes, which may seem insufficient to evaluate the effects of acupuncture. We attempted longer examinations in a preliminary study, but complete immobilization of the right forearm for more than 15 minutes was found to be difficult because of muscle strain and cramps.

There were 26 subjects enrolled in this study, but seven (26.9 %) did not yield reliable measurements of radial artery diameter during acupuncture due to the influence of forearm movements. Strict exclusion criteria were employed so that accurate data could be obtained. Because of this, however, it was difficult to perform the test repeatedly in the same subject, so we could not obtain data from a control intervention. Therefore, we only compared hemodynamics before and after acupuncture. In the future, we hope to compare the changes of radial artery blood flow volume with those after stimulation at another acupoint or after nonspecific stimulation.

Although we should view these results cautiously because this was a pilot study with a small sample size and no control intervention, the present findings suggest that acupuncture at a single acupoint can alter both radial artery hemodynamics and systemic hemodynamics in healthy subjects.

CONCLUSIONS

In conclusion, the present study showed that radial artery blood flow volume decreased immediately during acupuncture at the LR-3 acupoint, but increased by 180 seconds after acupuncture. We could assess quantitative changes of peripheral vessel hemodynamics accurately by using the present high-resolution ultrasound system with automated echo-tracking.

Acknowledgments

We thank T. Kamiya, A. Matsuda, and S. Kaneko, Department of Acupuncture Therapy, Tohoku University Hospital, for their technical assistance.

REFERENCES

1. Xu X. Acupuncture in an outpatient clinic in China: a comparison with the use of acupuncture in North America. *South Med J.* 2001; 94:813-816.
2. Napadow V, Kaptchuk TJ. Patient characteristics for outpatient acupuncture in Beijing, China. *J Altern Complement Med.* 2004;10:565-572.
3. Witt CM, Jena S, Brinkhaus B, Liecker B, Wegscheider K, Willich SN. Acupuncture for patients with chronic neck pain. *Pain.* 2006; 125:98-106.
4. Brinkhaus B, Witt CM, Jena S, et al. Acupuncture in patients with chronic low back pain: a randomized controlled trial. *Arch Intern Med.* 2006;166:450-457.
5. Linde K, Allais G, Brinkhaus B, Manheimer E, Vickers A, White AR. Acupuncture for tension-type headache. *Cochrane Database Syst Rev.* 2009;(1):CD007587.
6. Witt C, Brinkhaus B, Jena S, et al. Acupuncture in patients with osteoarthritis of the knee: a randomised trial. *Lancet.* 2005;366:136-143.
7. Linde K, Allais G, Brinkhaus B, Manheimer E, Vickers A, White AR. Acupuncture for migraine prophylaxis. *Cochrane Database Syst Rev.* 2009;(1):CD001218.
8. Wan WK, Hsu TL, Chang HC, Wan YY. Effect of acupuncture at Hsien-Ku (St-43) on the pulse spectrum and a discussion of the evidence for the frequency structure of Chinese medicine. *Am J Chin Med.* 2000;28:41-55.
9. Haker E, Egekvist H, Bjerring P. Effect of sensory stimulation (acupuncture) on sympathetic and parasympathetic activities in healthy subjects. *J Auton Nerv Syst.* 2000;79:52-59.
10. Syuu Y, Matsubara H, Kiyooka T, et al. Cardiovascular beneficial effects of electroacupuncture at Neiguan (PC-6) acupoint in anesthetized open-chest dog. *Jpn J Physiol.* 2001;51:231-238.
11. Boutouyrie P, Corvisier R, Azizi M, et al. Effects of acupuncture on radial artery hemodynamics: controlled trials in sensitized and naive subjects. *Am J Physiol Heart Circ Physiol.* 2001;280: H628-H633.
12. Bensky D, O'Connor J. *Acupuncture a Comprehensive Text.* Seattle, WA: Eastland Press; 1981:292-293.
13. Soga J, Nishioka K, Nakamura S, et al. Measurement of flow-mediated vasodilation of the brachial artery: a comparison of measurements in the seated and supine positions. *Circ J.* 2007; 71:736-740.
14. Burns PN, Jaffe CC. Quantitative flow measurements with Doppler ultrasound: techniques, accuracy, and limitations. *Radiol Clin North Am.* 1985;23:641-657.
15. Taylor KJ, Holland S. Doppler US. Part I. Basic principles, instrumentation, and pitfalls. *Radiology.* 1990;174:297-307.
16. Gill RW. Measurement of blood flow by ultrasound: accuracy and sources of error. *Ultrasound Med Biol.* 1985;11:625-641.
17. Deanfield J, Donald A, Ferri C, et al. Endothelial function and dysfunction. Part I: methodological issues for assessment in the different vascular beds: a statement by the Working Group on Endothelin and Endothelial Factors of the European Society of Hypertension. *J Hypertens.* 2005;23:7-17.
18. Corretti MC, Anderson TJ, Benjamin EJ, et al. Guidelines for the ultrasound assessment of endothelial-dependent flow-mediated vasodilation of the brachial artery: a report of the International Brachial Artery Reactivity Task Force. *J Am Coll Cardiol.* 2002;39:257-265.
19. Elie B, Guiheneuc P. Sympathetic skin response: normal results in different experimental conditions. *Electroencephalogr Clin Neurophysiol.* 1990;76:258-267.